

1-1-2013

Investigating The Metal Binding Affinity Of Bacterial Zinc Transporters: Zupt And Truncated Znta (znta-Pina)

Fei Nie

Wayne State University,

Follow this and additional works at: http://digitalcommons.wayne.edu/oa_theses



Part of the [Biochemistry Commons](#), and the [Molecular Biology Commons](#)

Recommended Citation

Nie, Fei, "Investigating The Metal Binding Affinity Of Bacterial Zinc Transporters: Zupt And Truncated Znta (znta-Pina)" (2013). *Wayne State University Theses*. Paper 269.

This Open Access Thesis is brought to you for free and open access by DigitalCommons@WayneState. It has been accepted for inclusion in Wayne State University Theses by an authorized administrator of DigitalCommons@WayneState.

**INVESTIGATING THE METAL BINDING AFFINITY OF BACTERIAL ZINC TRANSPORTERS: ZUPT
AND TRUNCATED ZNTA (ZNTA-PINA)**

by

FEI NIE

THESIS

Submitted to the Graduate School

of Wayne State University,

Detroit, Michigan

in partial fulfillment of the requirements

for the degree of

MASTER OF SCIENCE

2013

MAJOR: BIOCHEMISTRY AND
MOLECULAR BIOLOGY

Approved by:

Advisor

Date

DEDICATION

I would like to dedicate my thesis to my beloved parents.

ACKNOWLEDGMENTS

Firstly, I would like to thank the department of Biochemistry and Molecular Biology at School of Medicine of Wayne State University for giving me the opportunity to be a member of department and do projects. I would like to express my deepest appreciation to my advisor Dr. Bharati Mitra who mentored me and led me to be a biochemist. Without her guidance and help, this thesis would not have been possible.

In addition, I would like to thank my committee members, Dr. Timothy Stemmler and Dr. David Evans for being part of my committee, taking time to review my thesis, and guiding my research.

Finally, I would like to thank the previous lab members I have worked with Ashoka Kandegedara and Asmaa F. Adaba for their help during my research in the lab. Thanks again to all of you.

TABLE OF CONTENTS

Dedication.....	ii
Acknowledgement.....	iii
List of Tables.....	v
List of Figures.....	vi
Chapter1: Introduction.....	1
Chapter2: Investigating the metal binding affinity of recombinant ZupT.....	23
Chapter3: Investigating the metal binding affinity of PINA-ZntA.....	49
References.....	62
Abstract.....	69
Autobiographical Statement.....	70

LIST OF TABLES

Table 1.1: Selected chemical elements in the human body.....	1
Table 2.1 Different expression systems for ZupT.....	26
Table 2.2 ZupT expression optimization gradient.....	32

LIST OF FIGURES

Figure 1.1: Comparison of the effects of zinc excess vs. zinc deficiency in the human body.....	6
Figure 1.2: Intracellular zinc homeostasis in <i>S. cerevisiae</i>	8
Figure 1.3: <i>E. coli</i> intracellular zinc homeostasis.....	9
Figure 1.4 Mammalian zinc transporters.....	11
Figure 1.5 The catalytic cycle of Na ⁺ /K ⁺ ATPase.....	17
Figure 1.6: Predicted structure of ZupT.....	20
Figure 2.1: ZupT with strep tag in pBAD myc hisC vector.....	24
Figure 2.2: Wild type ZupT in the pASK IBA3 vector.....	25
Figure 2.3: Result of a ZupT family sequence alignment.....	30
Figure 2.4: Western blot comparing ZupT expression from different systems.....	31
Figure 2.5: Different fractions of noninduced and induced ZupT pASK IBA3/JM83.....	32
Figure 2.6: Western blotting results for optimization of ZupT expression.....	35
Figure 2.7: SDS gel with the fractions from a ZupT purification using a single strep-tactin column.....	36
Figure 2.8: SDS gel with the fractions from the ZupT purification for the combination of DEAE ion exchange column and strep-tactin column.....	38
Figure 2.9A: SDS gel with fractions of ZupT purification of combination of Talon column and strep-tactin column. Figure is the result for purification of Strep-tactin	

followed by Talon column.....	39
Figure 2.9B: Western blotting results of fractions of ZupT purification of combination of Talon column and strep-tactic column.....	40
Figure 2.10: SDS gel with the fractions from the ZupT purification of the combination of Ni ²⁺ column and strep-tactin column.....	41
Figure2.11: Emission spectrum of ZupT in the 300-500nm range with increasing amounts of added Zn ²⁺ ; the arrow shows the direction of fluorescence change.....	42
Figure2.12: Plot of relative change in fluorescence emission at 330nm from Figure 2.11 above as a function of the added zinc salt concentration.....	43
Figure2.13: Plot the absorbance change at 366 nm of mag-fura-2, and the data was fitted using Dynafit software.....	44
Figure2.14: 10% gel SDS gel result of different treatment of purified ZupT.....	46
Figure3.1: Predicted structure of ZntA(A) and PINA-ZntA(B).....	49
Figure3.2: SDS gel with the fractions from the PINA-ZntA purification using a combination of Ni ²⁺ column and strep-tactin column.....	53
Figure3.3: Emission spectrum of ZntA- PINA in the 295-500nm range with increasing amounts of added Pb ²⁺ ; the arrow indicates the direction of fluorescence change.....	54
Figure3.4: Emission spectrum of ZntA- PINA in the 295-500nm range with increasing amounts of added Cd ²⁺	55

Figure3.5: Emission spectrum of ZntA- PINA in the 295-500nm range with increasing amounts of added Zn^{2+}	56
Figure3.6: Plot of fluorescence change in fluorescence emission at 325nm from Figure 3.3 above as a function of the added lead salt concentration.....	57
Figure3.7: Determination of Zn binding affinity of PINA-ZntA using competition titration with mag-fura-2.....	58
Figure3.8: Cadmium titration with mag-fura-2 with or without PINA-ZntA present.....	59

CHAPTER 1

INTRODUCTION

All living organisms contain certain chemicals which are essential for living. Based on their relative amount in cells, these have been categorized into four major groups: (1) Bulk elements, (2) Macrominerals and ions, (3) Trace elements, (4) Ultratrace elements.¹

Table 1.1 Selected chemical elements in the human body¹.

Elements	Category	Percentage (by weight)
Oxygen	Bulk	53.6
Carbon	Bulk	16.0
Sodium, potassium	Macrominerals	0.10
Chlorine	Macrominerals	0.09
Iron	Trace elements	0.005
Zinc	Trace elements	0.003
Copper	Trace elements	2×10^{-4}
Manganese	Ultratrace elements	2×10^{-5}
Lead	Ultratrace elements	9×10^{-6}

Though each type of element is present in vastly different amounts they all play important roles in organisms. Bulk elements (O, C, N, H, P, and S) make up the basic composition for all the compounds necessary for organisms. Macrominerals such as sodium, potassium, magnesium, calcium, chlorine, and phosphorus provide essential ions to maintain osmotic balance or are

components of structural elements for organisms. Trace elements including iron, copper, zinc, are present in small amounts, and usually act as structural elements of enzymes in organisms or as catalytic cofactors. Ultratrace elements like manganese, nickel, and cobalt, which are present at less than 0.0001% by weight, play important roles in metabolism for organisms².

1.1 Transition metal homeostasis

Transition metals are a group of metals many of which can exist in several oxidation states, and usually participate in many important biological processes. They can act as electron carriers, and catalyze oxygen transport as well as key steps in enzyme catalysis. Transition metal such as Mn, Fe, Cu have several redox states, so they can serve as carriers for electron transfer reactions¹. Transition metals are essential for all living organisms. Most of the trace elements and ultratrace elements are transition metals, such as iron, copper, zinc, and nickel¹. Iron is the most abundant metal in eukaryotes, bacteria, and archaea: it serves as a cofactor in respiration and as a structural element in many proteins³. Zinc is another common transition metal for living organisms: it operates as a structural element to maintain proper protein folding; also it is important in gene regulation³. Nickel is usually present as a component of key enzymes for the final step of methane production in bacteria⁴.

Living organisms need transition metals for their metabolism and other biological processes; however, the concentration of transition metals in living organisms is usually tightly regulated in a narrow range, since excess transition metals are also toxic for organisms and can cause serious problems. Free metals ions are present under excess conditions; excess of a specific metal ion may affect uptake of another metal, and then affect its role in biological processes; some redox-active metals may cause oxidative damage for organisms when in excess^{1,4,7,8}.

When plants are under metal deficiency conditions, they increase metal uptake by activating high-affinity transporters and modifying the pathways for metal distribution. In contrast, when metals are in excess, plants will activate the mechanisms for intracellular chelation, compartmentalization, and expression of metallothioneins⁶.

Transition metals are also important for human beings. They act as cofactors for many key processes in the body, such as respiration, and serve as structural elements and catalytic centers for many key enzymes. Both deficiency and excess of metals cause many human diseases. For example, hemochromatosis is due to iron overload, while thrombocytosis results from iron deficiency. In order to maintain the optimum level of transition metals in the body, mechanisms of metal chelation, metal uptake, metal storage, and metal trafficking are involved in this complex process⁵.

1.2 Biology of Zinc

Zinc is a widespread element in living organisms, and it is the only transition metal to exist in all six classes of enzymes. Zinc is an essential component of more than 300 enzymes, which play critical roles in cell division, growth and differentiation, programmed cell death, gene transcription, biomembrane functioning and obviously many enzymatic activities and enzymatic structures⁵.

Zinc plays three major roles in enzymes: catalytic, structural and regulatory roles⁵. Zinc plays a catalytic role in many cell processes including DNA synthesis, normal growth, brain development, behavioral response, reproduction, fetal development, membrane stability, bone formation, and wound healing^{5, 6, 9}. Zinc also plays structural and functional roles in proteins to stabilize the protein fold, including proteins involved in DNA replication and reverse

transcription^{5, 6, 9}. For instance, in the transcription factors known as zinc finger proteins, a group of proteins that have zinc finger motif, zinc is required to stabilize the structure. Zinc can regulate protein stability and enzymatic activity as an activator or inhibitor. Zinc can also modulate cellular signal transduction processes and modulate synaptic neurotransmission in Zn-containing neurons in the forebrain⁵.

In living organisms, zinc exists in a paradox situation in that zinc as an essential nutrient plays important roles in many biological processes, while excess zinc is toxic since it is a potent disrupter of cellular processes via the following mechanisms. Firstly, Zn(II) is a strong Lewis acid and electron pair acceptor, compared to other intracellular metal ions except copper. Excess Zn(II) can block copper absorption and the activity of copper related enzymes. Secondly, Zn(II) can inhibit the formation of free radicals, so it can protect sulfhydryl groups. When the intracellular concentration of Zn(II) increases to toxic levels, it prevents disulfide bonds formation and disrupts the function of enzymes that need the help of disulfide bonds for structure and function^{5, 6, 9, 10}.

1.3 Zinc and Human Health

Zinc is ubiquitous in humans and is the second most abundant trace element in humans after iron. In humans, the average amount of Zn in adults is 1.4-2.3g, and the zinc concentration in plasma is 12-16 μM ¹¹. Most of the zinc is distributed in muscle, brain, skin, bones, kidney, and liver. About 85% of whole body zinc is present in muscle and brain, and about 11% exists in skin and liver⁵. Recent studies showed that about 10% of proteins in the human genome potentially bind zinc, and zinc is a cofactor for more than 300 enzymes in humans^{5, 9}.

Given the significance of zinc, disruption of zinc homeostasis leads to serious health problems in humans (Figure1.1). Zinc deficiency can lead to growth retardation, defects in

reproductive organs, dysfunction of the immune system and cognitive problems¹². Zinc deprivation can cause symptoms such as anorexia, loss of appetite, smell and taste failure, and may affect the immune system, triggering arteriosclerosis and anemia⁵. Increasing evidence shows that zinc deficiency is also involved in immunity disorders and in diseases such as cancer, diabetes, depression, as well as Wilson's disease, Alzheimer's disease, and other age-related diseases. Studies on mice suggest that dietary zinc supplementation prevents early onset diabetes in mice, and patients with Type 1 diabetes have significantly low intracellular zinc levels^{13, 14}.

Although zinc is important for the human body and lack of zinc can lead to serious health problems, excess zinc is also harmful for humans. As discussed above, excessive zinc absorption will lead to copper deficiency, since zinc can suppress the absorption of copper¹⁵. It is known that a large amount of zinc exists in glutamate synaptic vesicles in the mammalian forebrain. This zinc is released along with glutamate into the synaptic cleft during neuronal activity, and then taken up by post-synaptic cells. Long-term exposure to excess zinc will be toxic and damage the adjacent neurons¹⁶. Excess zinc is also involved in Alzheimer's disease (AD). Zinc is essential for enzymatic nonamyloidogenic processing of the amyloid precursor protein (APP) and enzymatic degradation of the amyloid- β ($A\beta$) peptide. Zinc can bind to $A\beta$ and promote its aggregation and precipitation resulting in synaptic and memory deficits¹⁷. Chelation of zinc has shown to reduce the formation of $A\beta$ plaques in animal studies¹⁸.

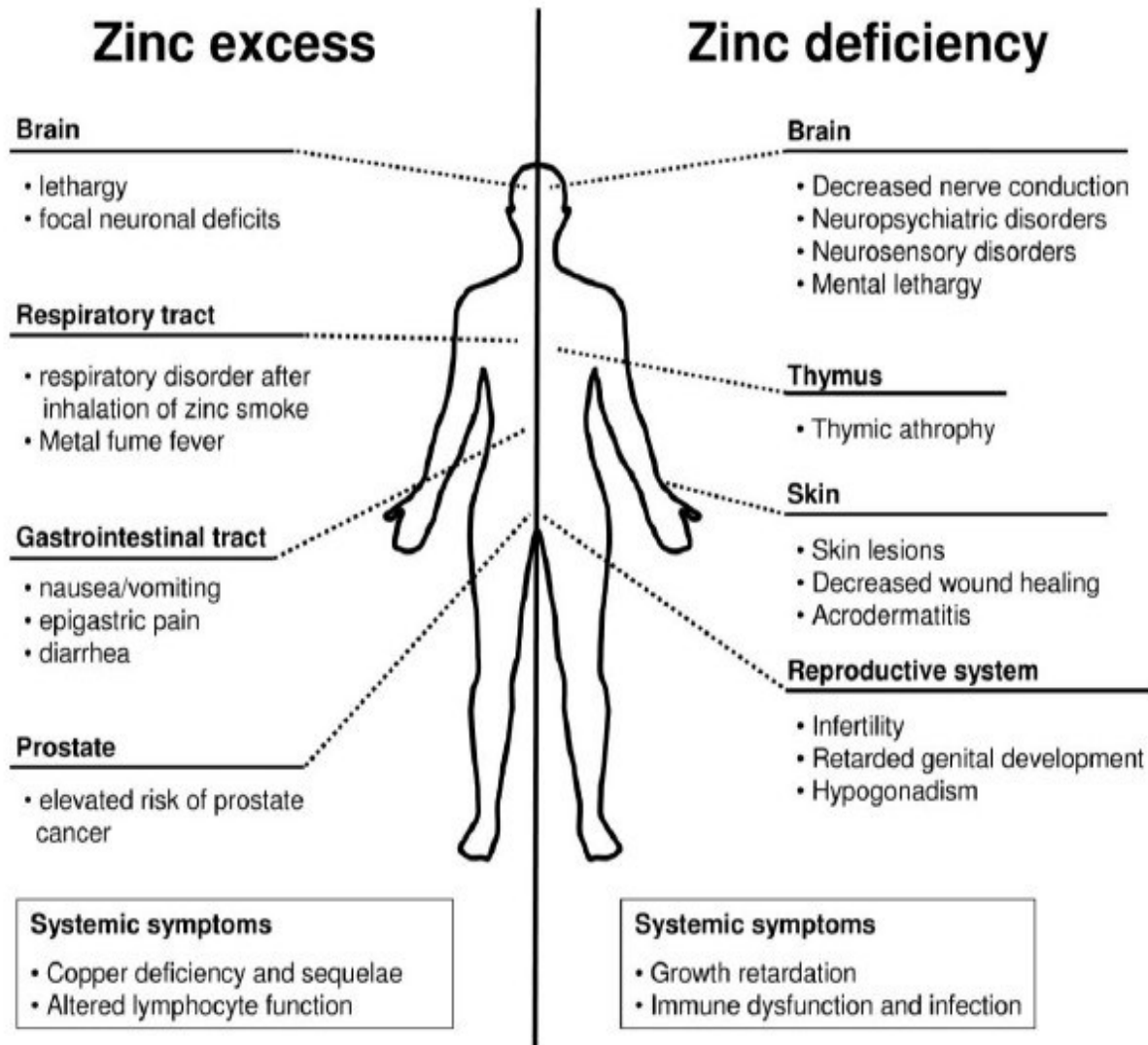


Figure 1.1: Comparison of the effects of zinc excess vs. zinc deficiency in the human body. Excess of zinc and deprivation of zinc are both harmful for different organ systems¹².

1.4 Cellular Zinc Homeostasis

Since zinc plays various roles in organisms, zinc levels are tightly regulated in cells. So what is the zinc level in cells? O' Halloran first proposed the "zinc quota", which is defined as the total zinc content required for its optimum growth²¹. The zinc quota of *Escherichia coli* is about 10^5 atoms of zinc per cell. In yeast, the zinc quota is about 10^7 atoms of zinc per cell. For some mammalian cell cultures the zinc requirement is about 10^8 atoms per cell for cell growth²².

^{23, 24}. Thus the zinc quota for different cell types is quite different. However, when the volume of these three different cell types is adjusted, the zinc concentration is similar, 0.1 to 0.5 mM²⁷. However, this is not always true. Certain types of cells such as some neurons, and prostate cells, have higher zinc concentration than other tissues; this may reflect the fact that zinc has a specialized role in these types of cells^{25, 26}.

From the data above, we know that cells can tightly control intracellular zinc level; but how do they do that? There is an extensive network of processes for regulation of intracellular zinc, which is carried out by zinc importers and exporters, cellular ligands, and transcription factors²⁷. Since the regulation system of zinc homeostasis is not the same in eukaryotic and prokaryotic cells, I will describe them separately.

In eukaryotic cells, transporters, cellular ligands, and transcription factors are all involved in the process of regulation of intracellular zinc homeostasis²⁷. For the situation of zinc repletion, cells can down-regulate zinc importers, increase the expression of zinc exporters and store the free zinc in loosely bound forms for future use, in order to keep the free zinc concentration at a nontoxic level. During zinc deficiency conditions, eukaryotic cells will up-regulate high affinity zinc importers, inhibit the expression of zinc exporters, and recruit the stored zinc to maintain the structure and function of zinc bound proteins²⁸. Some metallothioneins, which are a family of proteins that can bind to free metals, serve as both gene transcription factors to regulate the expression of transporters and cellular metal ligands to maintain intracellular zinc levels²⁸. The following Figure 1.2 shows the proposed intracellular zinc homeostasis regulation in yeast.

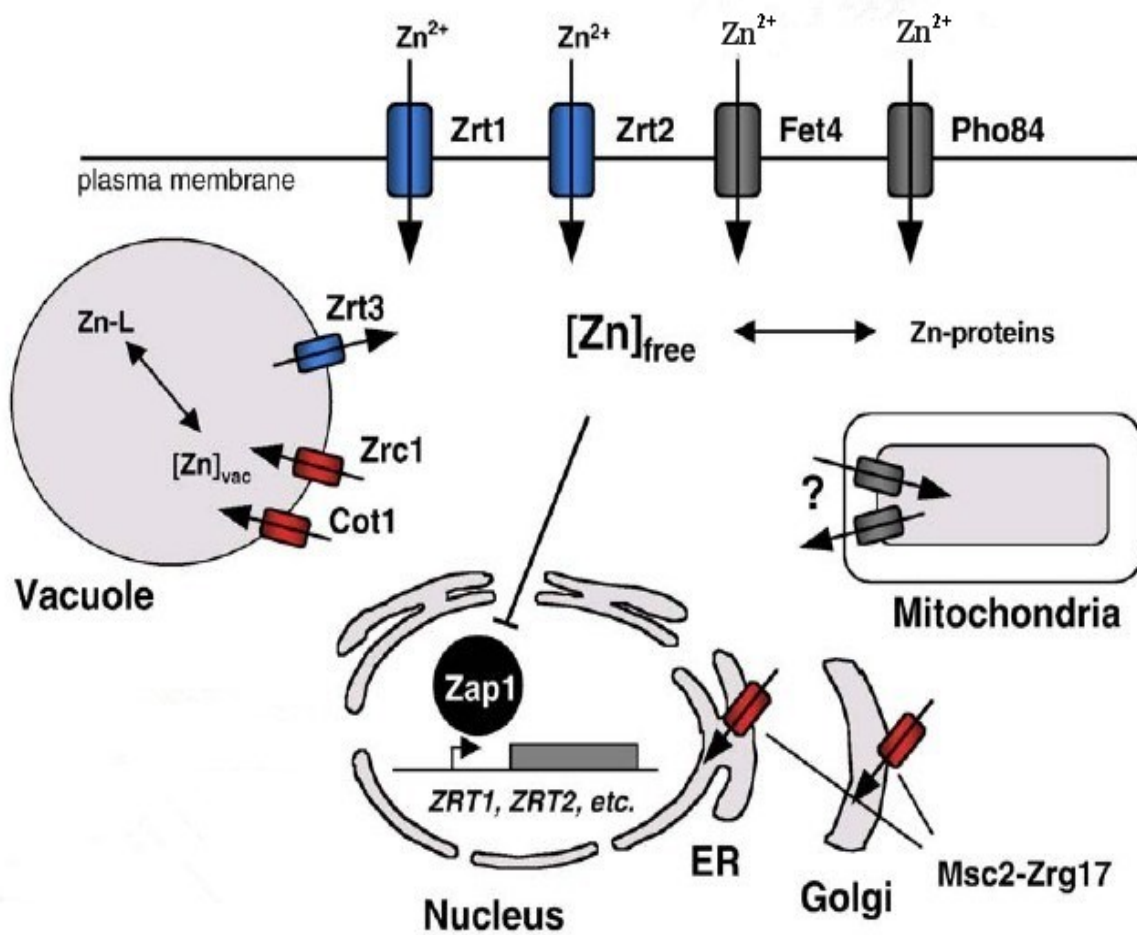


Figure 1.2: Intracellular zinc homeostasis in *S. cerevisiae*. During zinc limiting conditions, Zap1, a zinc-responsive activator protein, can up-regulate the expression of high affinity zinc importers Zrt1 and Zrt2. Fet4 and Pho84 are low affinity broad spectrum transporters that can transport other ions besides zinc. Zrt3, a vacuolar transporter, can facilitate zinc movement from vacuole to cytosol to maintain cytosolic zinc levels. For zinc replete conditions, Cot1 and Zrc1, transporters located on the vacuolar membrane, and Zhf located on the ER membrane, will transport zinc from the cytosol to vacuoles or ER. ZIP family transporters are shown in blue and CDF family transporters in red. Hypothetical and known transporters from other families are shown in gray²⁷.

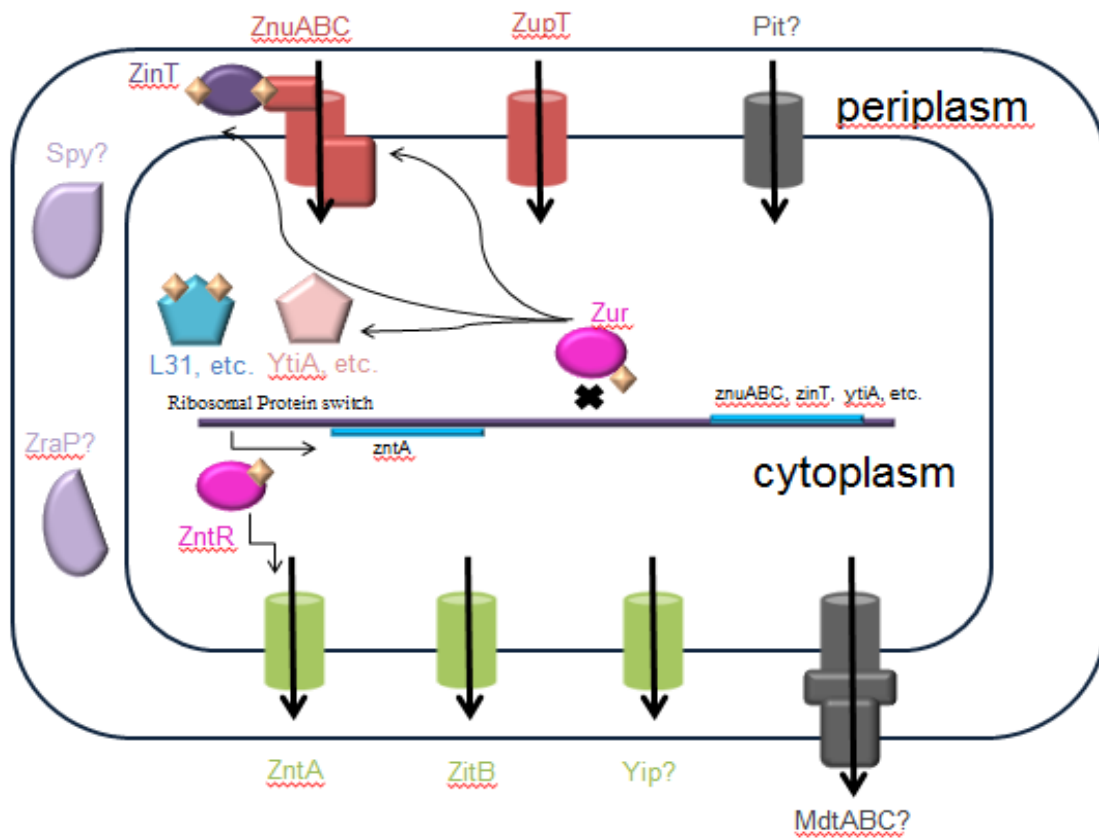


Figure 1.3: *E. coli* intracellular zinc homeostasis. Zinc homeostasis is mainly controlled by influx and efflux transporters. Under deficiency conditions, Zur, a Fur homolog transcription activator, activates the transcription of *znuABC* to up-regulate the high affinity zinc importer ZnuABC. ZupT, which is a low affinity zinc importer also imports zinc to the cytoplasm. PitA, a low affinity phosphate transporter, may also play a role in transporting zinc²⁸. When *E. coli* is under zinc stress, ZntA, ZitB, and YipP work together to remove the excess zinc from the cytoplasm. Ribosomal protein switches are also regulated by Zur to release zinc from other key cytosolic metalloproteins. ZitB and YipP are low affinity zinc exporters from the CDF family, while ZntA is a high affinity zinc exporter from the P-type ATPase family. ZntR, a zinc sensor, regulates the expression of ZntA²⁹.

In prokaryotic cells, intracellular zinc homeostasis is mainly regulated by import and export systems that are regulated by their own transcription factors separately²⁸. Storage mechanisms are also involved in bacterial zinc homeostasis²⁹. Bacterial cells need to be protected against dramatic zinc concentration changes in the environment. Under zinc-limited situations, bacterial cells will up-regulate and activate both high affinity and low affinity zinc importers. Under zinc stress, the cells will export zinc by up-regulation of zinc exporters^{28,29}. *E. coli* is the most popular prokaryotic model, and Figure 1.3 shows its intracellular zinc homeostasis.

1.5 Zinc Transporters

Zinc transporters are important for zinc homeostasis. Their role is to facilitate Zn movement through the membranes, in order to maintain optimal Zn levels in cells. Zinc transporters belong to different transporter families: RND multi-drug efflux transporters, P-type ATPases, ABC transporters, the ZIP (Zrt-, Irt-like Protein) family, and the CDF (cation-diffusion facilitators)/ZnT family of zinc transporters^{27, 28}. However, these transporter families are not ubiquitous. In eukaryotic cells, zinc transporters mainly come from the ZIP family and CDF/ZnT families. RND transporters and ABC transporters have been reported to only exist in bacteria, and only a few P-type ATPase family members play a role in transporting metal ions in eukaryotes^{27,28}. Here, I will introduce these five transport families.

1.5.1 Mammalian Zinc transporter families

As mentioned above, mammalian zinc transporters mainly come from two families: ZIP (Zrt- and Irt-like proteins) [solute-linked carrier 39 (SLC39)] and ZnT proteins [solute-linked carrier 30 (SLC30)]³⁰. For humans, zinc transporters are named as SLC39A1 or SLC30A1, etc. Members of these two families have opposite roles in cellular zinc homeostasis. Zip transporters increase cytoplasm zinc levels by uptake of zinc from extracellular space or transporting

vesicular zinc to the cytoplasm, while Znt transporters reduce intracellular zinc by exporting zinc to extracellular space or organelles (Figure 1.4).

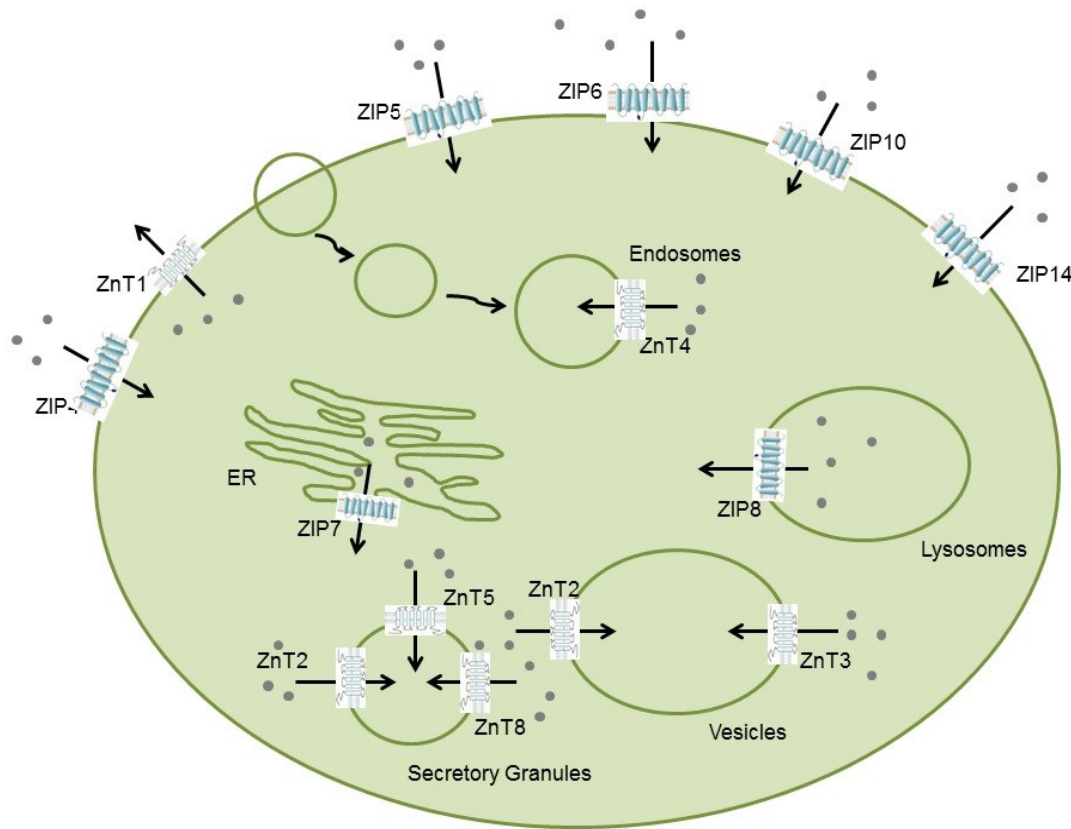


Figure 1.4 Mammalian zinc transporters. This figure shows the location and the function of some key zinc transporters in a mammalian cell. The arrows also show the direction of zinc movement for each transporter. As shown, the function of Zip and ZnT transporters is to increase and decrease intracellular zinc concentration³⁰, respectively.

1.5.1.1 ZIP Transporter family (SLC39)

The ZIP (Zrt, Irt-like protein) family is named after the first members discovered: IRT1 in *Arabidopsis thaliana*³², and ZRT1 and ZRT2 in *Saccharomyces cerevisiae*^{33,34}. Members from this family are widely present in bacteria, fungi, archaeae, plants and mammals³¹. The mammalian

members in this family are also named as SLC39³⁵. Members of the ZIP family play roles to increase cytoplasmic zinc concentration by transporting zinc from extracellular space or organellar lumen into the cytosol. ZIP transporters mainly transport zinc, however, they are also involved in iron, manganese and cadmium transport³⁰. There are fourteen zinc transporters belonging to the ZIP family in humans (Figure 1.4). Most members in this family are predicted to have eight transmembrane domains (TMDs) and similar topologies, with both N-terminal and C-terminal ends of the protein located on the extracellular side of the membrane. Many members have a long loop between TMDs 3 and 4, and a histidine-rich region is also located on this loop. The function of this domain still not known, however, given the potential metal binding ability, it may play a role in zinc binding or in regulation of transport³⁰. Also the alignment result showing sequence conservation on TMDs 4 and 5 suggests this may be the channel for passage of the metal through the membrane³⁰.

Based on sequence conservation, the ZIP family can be divided into four subfamilies : I, II, LIV-1, and *gufA*^{31, 36}. Members in subfamily I are mainly from fungal and plant sources, while subfamily II consists of mammalian, nematode and insect genes. In humans, there are 4 zinc transporters belonging to these two subfamilies: hZIP9 belong to ZIP subfamily I, and hZIP1, hZIP2, and hZIP3, all belong to ZIP subfamily II. Members in subfamily I and II are predicted to have eight transmembrane domains, and the N-terminus and C-terminus of these transporters are located outside the plasma membrane^{31, 36}. There is a variable region present between TMs 3 and TMs 4 of transporters from these subfamilies that is located in the cytoplasm. This region has little sequence homology among the subfamily members, however, there is a His-rich portion in this region which is predicted to be the zinc binding domain^{31, 36}. Between TMs IV and TMs V, there are two highly conserved portions that are amphipathic and contain

conserved His residues among the members^{21, 37}. These two portions are considered to form a channel where the zinc ions can pass through and the conserved His residues or adjacent polar residues serve as an extramembrane metal ion binding sites in these proteins³⁷. In support of this hypothesis, mutations of conserved His residues and adjacent polar residues in TMs IV and TMs V of IRT1 were shown to abolish transporter activity³⁸.

The LIV-1 subfamily, which is also named LZT (LIV-1 subfamily of ZIP zinc Transporters), is distinguished by the conserved metalloprotease-like sequence HEXPHEXGD in TM V³⁹. Members in this subfamily usually have a large N-terminal sequence compared to other ZIP family members. However, the membrane topology of the LIV-1 subfamily is still in controversy. Some reports predict there are 6 to 8 TMs, some believe it is 7 TMs, but generally researchers believe it has 8 TMs like transporters from other subfamilies^{39, 40, 41}. Currently there are 9 of human zinc transporters, hZIP4, hZIP5, hZIP6, hZIP7, hZIP8, hZIP10, hZIP12, hZIP13, hZIP14, belonging to this family.

The last subfamily is the *gufA* subfamily, which is related to the *gufA* gene of *Myxococcus xanthus*, and its function is still unknown. Only one human zinc transporter belongs to this subfamily: hZIP11.

1.5.1.2 ZnT Transporter family (SLC30)

ZnT transporters are also named as CDF (cation-diffusion facilitators) transporters. ZnT transporters have opposite roles compared to ZIP transporters; they serve to export intracellular zinc to extracellular space or to organelles. Members belonging to this family come from diverse organisms from fungi and bacteria to plants and mammals^{31, 36, 42-25}. To date, more than 100 members are found to belong to this family, and there are 8 human zinc transporters belonging to this family, ZnT1 to 8³⁰. Based on the sequence similarity, members in this family have been

divided into three subfamilies, ZnT subfamily I, II, and III³¹. Subfamily I contains most of the prokaryotic transporters, while subfamily II and III contain prokaryotic and eukaryotic transporters, and all of the human ZnT transporters belong to subfamily II and III³⁰. Most of ZnT transporters have similar membrane topology with 6 transmembrane domains and both C-terminal and N-terminal domains on the cytoplasmic side. However, some of these transporters are different from the majority, for example, hZnT5 has 15 transmembrane domains, and the yeast MSC2 has 12 transmembrane domains^{31, 42, 46}. Transporters in this family also have a His-rich loop that is located between TMs IV and TMs V^{31, 42, 46}. Additionally, TMs I, II, V, and VI are amphipathic transmembrane domains, and have been predicted to be composed of an inner core forming a channel and the remaining hydrophilic transmembrane domains III and IV are located on the outer shell. The three highly conserved Asp residues in transmembrane domain II, V, VI are predicted to be the zinc-binding site inside the channel⁴².

1.5.2 Bacterial Zinc transporter families

As mentioned above, Zinc transporters come from different transporter families: RND transporters, P-type ATPase family, ABC transporters, the ZIP family, and the ZnT family^{27, 28}. In mammalian cells, the zinc transporters mainly belong to the ZIP and ZnT families. However, in bacteria all of the above zinc transporter families have been shown to be involved in zinc homeostasis. The ZIP and ZnT families have been introduced above; the other three zinc transporter families are described below.

1.5.2.1 P-type ATPases family

P-type ATPases, named after a catalytic intermediate that is a key conserved aspartate residue phosphorylated during the reaction cycle, is a large superfamily of integral membrane proteins and are present in eukaryotes, archaea and bacteria^{47, 48, 49}. Based on the sequence

homology and substrate specificity, P-type ATPases are classified into five subfamilies, Type I to Type V, and each subfamily is further classified into subgroups on the basis of substrate specificity^{51, 58}. They pump ions and lipids across cellular membranes to generate ion gradients, which are important for a variety of cellular functions like signaling, energy storage and secondary transport^{47, 48, 49}. The first P-type pump, Na⁺/K⁺ ATPase, was discovered in the 1950s. Through the years, many other pumps with similar characteristics have been discovered and some of them are well studied and documented, such as Na⁺/K⁺ ATPase, Ca²⁺-ATPase, and H⁺/K⁺ ATPase^{47, 48, 49}. Studies on these pumps revealed many details about the structure and mechanism of this transporter family. P-type ATPases contain functionally and structurally distinct domains: a phosphorylation domain, an actuator domain, a nucleotide binding domain, a transport domain, and class specific support domains^{50, 51}.

The phosphorylation (P) domain as a central part of the cytoplasmic domain, is a highly conserved domain among all the P-type ATPases, and it contains a DKTGTLT motif. An Asp residue in this motif is phosphorylated reversibly during the ion transport. In the calcium pump, the P-domain assembles into a seven-stranded parallel β -sheet with eight helices forming a typical Rossman fold⁵⁰.

The actuator (A) domain is a highly conserved cytoplasmic domain; it contains the TGES motif, which is a conserved motif involved in dephosphorylation of the phosphorylated intermediate. Structural studies suggest that the domain contains a distorted jellyroll structure and the TGES motif is located at the edge of this domain. During the ion transport process, the A-domain especially the TGES motif, comes close in contact with the phosphorylation domain⁵⁰,

⁵¹.

The nucleotide binding (N) domain is essential for ATP binding and P-domain

phosphorylation. The N-domain is connected to the P-domain by a narrow hinge⁵⁰. It is the most variable cytoplasmic domain compared to the P-domain and A-domain. Nevertheless, the core structure of this domain is conserved⁵¹.

The transport (T) domain contains six membrane-spanning segments and protects the ion binding sites, and is located halfway through the membrane. This domain moves during the catalytic cycle to allow ions to associate and dissociate with the ion binding sites, so this domain is highly flexible^{50, 52, 53}.

The support (S) domain is a unit that can give structural support to the T-domain and has specialized functions like providing ion-coordinating side chains as additional ion binding site in some P-type ATPases such as Na^+/K^+ - and Ca^{2+} -ATPases. Compared to the T-domain, the S-domain is more rigid, and does not change much during the catalytic cycle⁵³.

Members of the P-type ATPases superfamily share a common mechanism for ion pumping. Here, I will use Na^+/K^+ pump as a model to demonstrate the catalytic mechanism (Figure 1.5). There are two distinct forms of the phosphorylated Na^+/K^+ -ATPase^{54, 55}: one is the phosphorylated form resulting from the addition of ATP and release ADP, $\text{E}_1\text{-P}$ (Enzyme₁-P), which is insensitive to K^+ ; the other one is sensitive to K^+ but not ADP, $\text{E}_2\text{-P}$ (Enzyme₂-P)⁵⁶. E_1 is phosphorylated to form $\text{E}_1\text{-P}$ when three intracellular Na^+ ions bind to the pump and release ADP. The phosphorylation leads to a conformational change in the pump to exposes the Na^+ ions to extracellular space. In the meantime, $\text{E}_1\text{-P}$ has low affinity for Na^+ ions, so it releases the Na^+ ions to extracellular space and the pump changes to the $\text{E}_2\text{-P}$ form. When two extracellular K^+ ions bind to $\text{E}_2\text{-P}$, $\text{E}_2\text{-P}$ will be dephosphorylated and revert to its previous conformation, E_2 , and expose the K^+ ions to intracellular space. The conformation reversal also lowers the affinity for K^+ ions. After releasing the K^+ ions, the pump is back to E_1 form again and ready to start another

catalytic cycle⁵⁷.

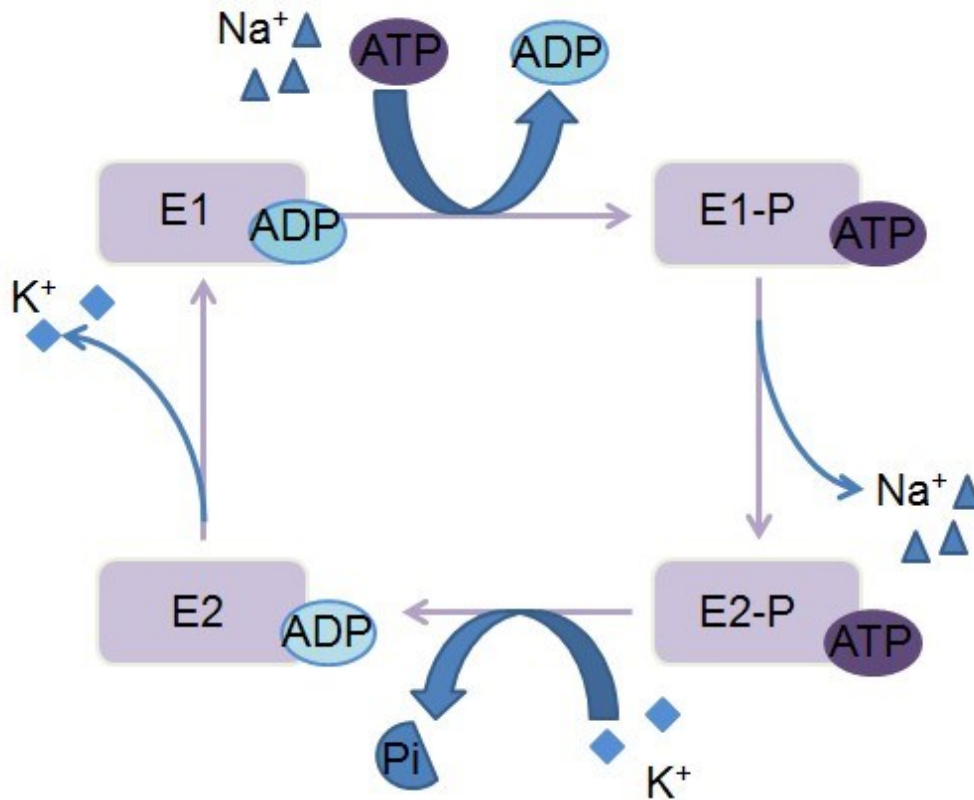


Figure 1.5 The catalytic cycle of Na⁺/K⁺ ATPase⁵⁷. All P-type ATPases follow the same mechanism as described above, and all domains work together to facilitate the ion transport.

1.5.2.2 RND (resistance-nodulation-cell division) transporter family

RND-driven tripartite protein complexes, which only exist in prokaryotes and not in eukaryotes, can efflux a wide array of substrates. The RND (resistance-nodulation-cell division) protein superfamily can be classified into seven protein subfamilies on the basis of substrate specificity⁶⁰. The RND transporters for Zn²⁺ are only found in few gram-negative bacteria²⁸. For example, CzcD protein of *Ralstonia metallidurans* is predicted to be first line of defense against high concentrations of Zn²⁺, since the *czcD* mutant strain is slightly more sensitive to Zn²⁺ than

the wild type strain⁵⁹. The CzcABC complex can export zinc ions, cobalt ions, and cadmium ions, across both cytoplasmic and outer membranes⁵⁹.

1.5.2.3 ABC (ATP Binding Cassette) transporter family

ATP binding Cassette transporters exist in all species, and they transport ligands across cellular lipid membranes, which is important for cell physiology. Transporters in this family can import metal ions such as zinc; in addition, they are also involved in nutrient uptake, resistance to cytotoxic drugs and antibiotics, and cholesterol and lipid trafficking²⁷. ABC transporters are a complex of three proteins, one or two of them are transmembrane proteins which can form a pore in the membrane allowing specific substrates to pass through the membrane⁶¹. Energy from ATP hydrolysis is required for the transport process⁶².

1.6 Zinc Transporters in *E. coli*.

Escherichia coli is a very good model system for zinc transporter studies. Our lab has used this system to study metal transporters for several years. The reason we use this model system is the whole genome of *E. coli* is well known and the strains are well adapted to the laboratory environment. In addition, *E. coli* has both high-affinity and low-affinity transporters working together to maintain the intracellular zinc homeostasis (Figure 1.3). There are four major zinc transporters from four different transporter families in *E. coli*: ZntA, ZitB, ZupT, and ZnuABC^{28, 29}.

1.6.1 Zinc exporters in *E. coli*

E. coli has both a high-affinity exporter, ZntA, and a low-affinity exporter ZitB²⁸. The zinc transporting ATPase (ZntA) belongs to the P-type ATPase superfamily, and it was originally identified by our lab^{71, 72, 73}. When the intracellular zinc concentration is high, ZntR, a zinc sensor, activates the expression of ZntA to transport the excess zinc to extracellular space⁶³.

ZitB, a low-affinity zinc exporter, belong to the CDF family⁶³. Sequence analysis and site specific mutagenesis studies suggest residues His53, His159, Asp163 and Asp186 are important for the transport process in ZitB⁶³. Additionally, these residues are conserved in the CDF transporter family, even when the specific substrates are different, suggesting these residues may form a proton channel⁶⁴.

1.6.2 Zinc importers in *E. coli*

E. coli also has both high-affinity and low-affinity zinc importers: ZnuABC and ZupT²⁹. ZnuABC, which belongs to the ABC transporter family, is induced by Zur, when the intracellular zinc concentration is extremely low. ZnuABC is a protein complex consisting of ZnuA, ZnuB and ZnuC. ZnuA is located on the periplasmic side, and binds to metal ions and ATP. ZnuB is the membrane permease and ZnuC is the subunit responsible for ATP hydrolysis⁶³. ZupT is a low-affinity zinc importer, which belongs to the ZIP family¹⁹. ZupT is a broad-spectrum zinc transporter, and can transport Fe^{2+} , Co^{2+} , Mn^{2+} and Cd^{2+} , besides Zn^{2+} ^{19, 65}.

1.7 Background of ZupT

ZupT is a cytoplasmic membrane protein, which is the first characterized ZIP family member protein in bacteria. Grass's report in 2002 showed that there is a low affinity zinc transporter, ZupT, which is responsible for zinc uptake in *E.coli*¹⁹. In addition, as a member of the ZIP transporter family, ZupT is a broad spectrum transporter that can transport iron and cobalt besides zinc, and possibly manganese and cadmium¹⁸. Like other ZIP transporters, ZupT is predicted to have eight transmembrane domains with both the N-terminal and C-terminal ends of the protein located on the extracellular side of the membrane³⁰ (Figure 1.6).

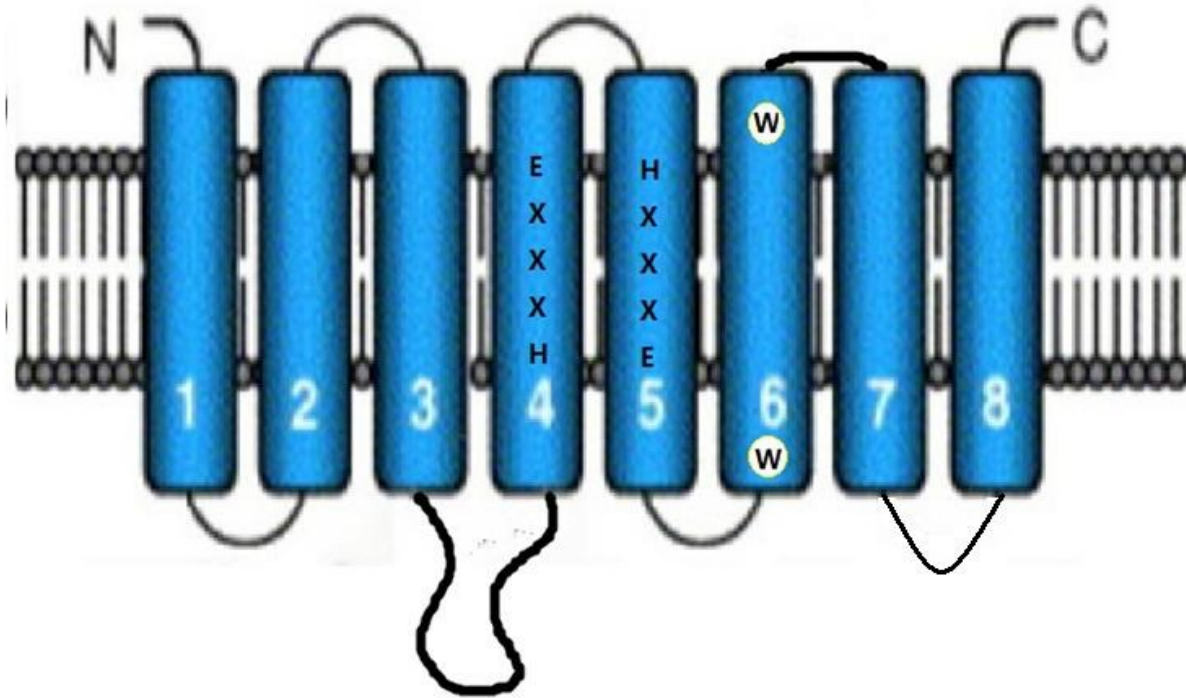


Figure 1.6: Predicted structure of ZupT

ZupT is also involved in some human diseases, for example, urinary tract infection²⁰. ZnuABC and ZupT play important roles in bacterial growth in Zn limiting condition during mouse urinary tract infection. The report also indicated that Znu was the primary zinc transporter, and loss of Znu and ZupT has effects on fitness during UTI²⁰.

Several reports had showed that ZupT is a broad spectrum metal transporter⁶⁵. It can transport iron besides zinc. *E. coli* strains with deletions in known iron uptake transporters were created, and the strains could grow in presence of chelators when ZupT is expressed while other iron importers were dysfunctional⁶⁵. Transport was studied with the deletion strains. The results suggested that ZupT can transport iron⁶⁵. Similar experiments were done for Co^{2+} , and the result suggests that ZupT can mediate Co^{2+} uptake⁶⁵. In addition, overexpression of ZupT makes the strain hypersensitive to Co^{2+} and Mn^{2+} ⁶⁵. All the results above suggest that ZupT is a broad

spectrum metal transporter, and it can transport iron, cobalt and manganese besides zinc. Transport studies from another group showed ZupT may also be involved in cadmium transport⁶⁶.

Competition experiments with other substrate cations for ZupT suggested that ZupT has a slight preference for Zn^{2+} , and the kinetic parameters for zinc also support this observation⁶⁶. ZupT can also transport Cu^{2+} ⁶⁶. Amino acid alignment results revealed several conserved residues that are located on TMs V and TMs VI⁶⁶. Site-specific mutagenesis has been done on some residues. Mutants H89A lead to loss of the ability to transport Co^{2+} and Fe^{2+} , while the S117V mutant cannot transport Mn^{2+} . In addition, E152D lost the activity to transport Zn^{2+} and Mn^{2+} ⁶⁶.

The studies mentioned above helped to solve a few of the mysteries about ZupT, however, there are still many unsolved questions, such as metal binding, coordination, geometry and ion selectivity of ZupT. My study will try to address some of these questions.

1.8 Background of PINA and ZntA-PINA

The pineal gland is a small endocrine gland in the brain, which is responsible for melatonin synthesis and secretion at night⁶⁹. Pineal night-specific ATPase (PINA) is a novel splice variant of the ATP7B gene; defects in ATP7B cause Wilsons disease⁶⁸. Wilsons disease is an inherited disorder of copper transport, and leads to copper accumulation in tissues⁷⁰. This disease is due to mutations in the ATP7B gene, which encodes a copper transporting ATPase belonging to the $\text{P}_{1\text{B}}$ subfamily of P-type ATPases. The sequence analysis result shows that PINA is identical to the C-terminal portion of ATP7B⁶⁸. Compared to ATP7B, PINA lacks the entire N-terminal domain, which contains six CXXC motifs important in copper binding, as well as the first four of eight transmembrane helices⁶⁸. However, PINA still retains important domains of P-type ATPases such as the phosphorylation domain, ATP binding domain, and the conserved CPC

motif. Indirect in vivo studies suggested that although the N-terminal copper binding region and 4 TMs are missing, PINA was still able to transport copper in yeast system but with much lower activity⁶⁸. So far, there is no direct evidence for transport activity of PINA.

ZntA, the high affinity zinc exporter in *E. coli*, another member of P_{1B} subfamily of P-type ATPases, can transport zinc, lead and cadmium⁶⁷. ZntA has two metal binding sites, one is in the N-terminal region and the other is in the transmembrane region⁶⁷. ZntA also has eight transmembrane domains, and since ZntA and ATP7B belong to the same subfamily, they may share the same mechanisms for metal transport. Although our lab has studied ZntA for several years, very little is known about the first four transmembrane helices. With the discovery of PINA, we wanted to test a similar truncated transporter, PINA-ZntA, which lacks the N-terminal domain and the first four transmembrane domains of ZntA, in order to investigate whether the rest of the transporter is still functional or not.

CHAPTER 2

INVESTIGATING THE METAL BINDING AFFINITY OF RECOMBINANT ZUP T

2.1 Purpose

As described in Chapter 1, ZupT belongs to the ZIP super family, members of which are metal importers. Previous studies have all been indirect and showed that ZupT can transport zinc, iron, cobalt, possibly cadmium, and manganese. However, the full metal selectivity for ZupT is still unknown. Therefore, the purpose of this study is to express and purify the recombinant protein, ZupT, in *E. coli*, and investigate its metal binding stoichiometry and affinity.

2.2 Materials

Plasmid pBAD/ myc hisC was purchased from Invitrogen. The ZupT pASK IBA3/JM83 strain was a gift from Dr. Sylvia Franke.

2.3 Methods

2.3.1 Construction of strep-tagged ZupT

ZupT strep (ZupT with a C-terminal eight residue-strep tag) was made by PCR using ZupT pBAD myc hisC as template, and the forward primer 5'-CGG CCA TGG CAG TAC CTC TC - 3', and the reverse primer 5'-CGG AAT TCT TAT TTT TCG AAC TGC GGG TGG CTC CAA CCA ATT CCC GC -3'. The PCR products and the pBAD myc hisC vector were digested with NcoI and EcoRI, and purified by using Gene Clean kit, and then the two fragments were ligated with T4 ligase. The ligation product was transformed into LMG194 competent cells. The sequence was verified by DNA sequencing.

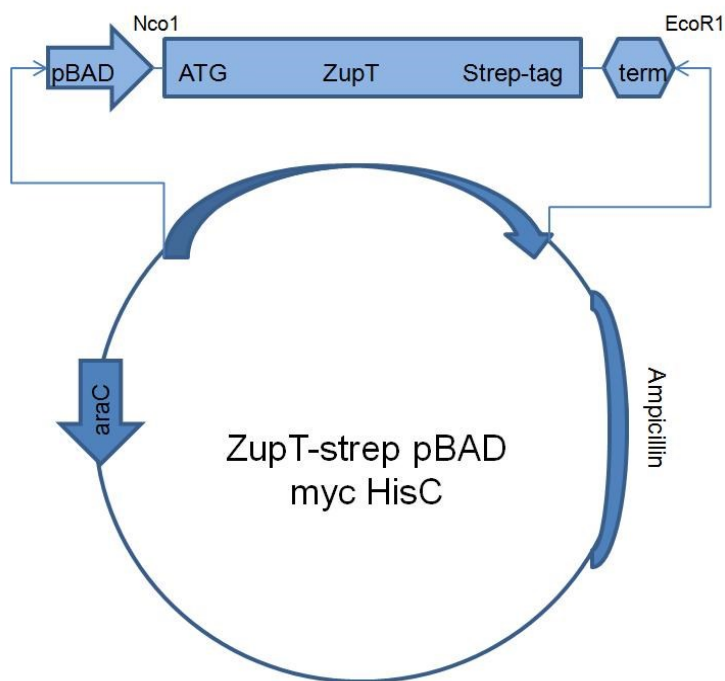


Figure 2.1 ZupT with strep tag in pBAD myc hisC vector.

2.3.2 Mutants of ZupT in pASK IBA3 vector.

A sequence alignment of ZupT and homologues from other species was performed by using CLUSTALW2 Multiple Sequence Alignment (European Bioinformatics Institute). The result shows there are two highly conserved regions: one region is in the fourth transmembrane helix; the other one is in the fifth transmembrane domain (Figure 2.2). Based on this observation, we assume that those two regions may play a role in the metal transport process. In order to investigate the metal binding sites, several ZupT mutants were created.

A previous lab member created four mutants H119N ZupT, E123Q ZupT, H148N ZupT, and E152Q ZupT in pBAD vector with a C-terminal His-tag. Since I observed that the best protein expression was from the ZupT pASK IBA3 construct (as explained later), I moved all the

mutants to the pASK IBA3 vector. The four mutants were subcloned from the pBAD constructs by PCR using the forward primer 5'- CCG AAT TCC TCA TTG TGA CCA TAC TGG C -3' and the reverse primer 5'- GGG CCT GCA GAC CAA TTC CCG CCG -3', used to create the original pBad/ZupT clone. Then using the restriction enzymes *EcoR*I and *Pst*I, the four PCR products were cloned into pASK IBA3. The constructs were then transformed into JM83 competent cells, and their sequences verified with sequencing by genewiz.

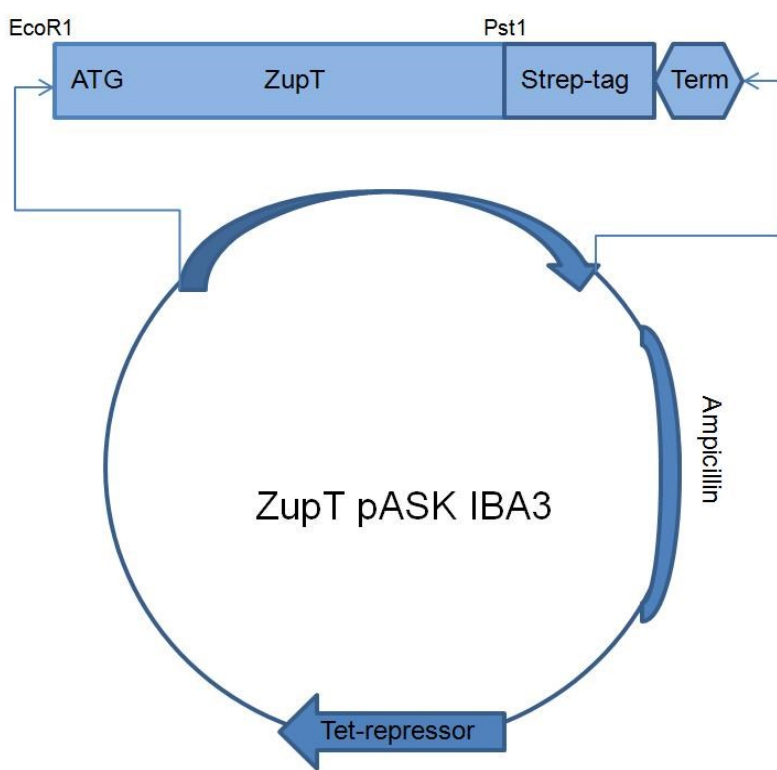


Figure 2.2 Wild type ZupT in the pASK IBA3 vector.

2.3.3 Optimization of ZupT expression.

ZupT is a membrane protein, and previous studies in our lab suggested the expression level for this protein is extremely low. Therefore, optimizing the ZupT expression was my first

task. Several expression systems were used, together with the strains listed in table 2.1. First, all the strains in the correct media were grown and each strain induced in mid-log phase with the appropriate inducer. After the appropriate time for induction, the cells were harvested and the expression level checked by western blotting.

Table 2.1 Different expression systems for ZupT.

Constructs	<i>E. coli</i> Strain	Media
ZupT-Strep pBAD myc hisC	LMG194	LB medium, LB medium+ Glycerol, M9 medium, Auto induction
	TOP10	
pSumo-ZupT	BL21	LB medium, LB medium+ Glycerol, M9 medium
ZupT pASK IBA3	JM83	
	BL21	

Based on the western blotting result, I chose the best expression system, and then optimized expression further by varying the OD₆₀₀ at which the cells were induced, the concentration of inducer, the induction temperature, and the induction time. Finally, the expression was checked by western blotting.

2.3.4 ZupT expression and purification

A single colony was used from a freshly-streaked LB/Amp plate to inoculate 5ml LB culture containing 100ug/ml ampicillin to OD₆₀₀=0.10. 1ml of this culture was used to inoculate 125ml LB culture with 100ug/ml ampicillin and grown overnight at 37°C. 10mL of the overnight culture was inoculated in 1L freshly-prepared LB media, and grown at 37°C about 3.5 hours until the OD₆₀₀ reach 0.8. The inducer, anhydrotetracycline (AHT), was added at this point (200ng/L)

to the culture. After 4 hours induction, the final OD₆₀₀ reached about 1.5. The cells were harvested by centrifugation (8500 rpm, 10 min) and stored at -20°C until further use.

The pellet was resuspended at 0.2g/mL in buffer A (25mM Tris-Cl pH7.0, 100mM Sucrose, 1mM PMSF). The cells were lysed by passage through a French press twice at 20,000 p.s.i. The cell suspension was incubated with DNaseI (0.02mg/mL) and 2mM MgCl₂ at 4°C for 40 minutes to degrade the chromosomal DNA. The cell debris was removed from lysed cells by low speed centrifugation (7500rpm, 30 min) at 4°C. The broken cells were centrifuged at high speed in an ultracentrifuge (45K rpm, 1h) at 4°C to separate the membrane proteins from soluble proteins. The membrane pellet was stored at 4°C (short term) or -20 °C (long term) till further use. The membrane pellet was resuspended in buffer B (25mM Tris-Cl pH7.0, 100mM Sucrose, 500mM NaCl, 1mM PMSF, 1mM 2-BME) to OD₂₈₀= 100, then Triton X-100 was added to final concentration 2% and the suspension stirred at 4°C for 1h. After solubilization, the suspension was centrifuged (45Krpm, 40min) to remove the insoluble fractions from solubilized proteins. The supernatant from the second ultracentrifugation was then loaded on a Ni²⁺-resin column pre-equilibrium with buffer C (25mM Tris-Cl pH7.0, 100mM Sucrose, 500mM NaCl, 1mM PMSF, 1mM 2-BME, 2mM DDM). The column was then washed consecutively with 5 column volumes of buffer C, and 5 column volumes buffer C with 10mM imidazole, and then the protein was eluted with 3 column volumes buffer C with 50mM imidazole. The eluted protein fractions were concentrated using 10K centricons, and then loaded onto the strep-tactin column pre-equilibrated with NP buffer (50mM NaH₂PO₄ pH8.0, 300mM NaCl, 2mM DDM). The column was washed with 5 to 10 column volumes NP buffer, and then the protein eluted with 20mL NPD buffer (NP buffer + 2.5mM desthiobiotin). 1mL fractions were collected, and the protein containing

fractions were checked using a crude Bicinchoninic acid assay (Sigma). Then all protein-containing fractions were combined, and concentrated using centricons. In order to remove the desthiobiotin, the concentrated protein was passed through a 20ml G-25 column with buffer D (10mM Bis-tris pH7.0, 2mM DDM). Protein-containing fractions were collected, pooled and concentrated again. 10% glycerol was added and aliquots of the protein stored at -80°C till further use.

2.3.5 Determination of protein concentration

Protein concentration was determined by using the bichinchonic acid assay with bovine serum albumin as standard. The principal for the bichinchonic acid assay is that Cu^{2+} ion is reduced by proteins to form Cu^{+} in alkaline condition. The amount of reduction is in direct proportion to the amount of protein present, and Cu^{+} and bichinchonic acid form a purple-blue complex, which has a maximum absorbance at 562nm. A standard curve is generated by using different concentration of bovine serum albumin.

2.3.6 Determination of the stoichiometry of ZupT by ICP-MS

The purified ZupT-strep was used to determine the concentration by BCA. Then 10uM ZupT-strep sample in buffer 10mM Bis-tris with 2mM DDM was incubated with 150uM Zn^{2+} at 4°C for 1 hour. The excess metal was removed by two consecutive passages through a G-25 gel filtration column. Protein-containing fractions were determined using BCA, and the fractions collected and concentrated using 10K Da centricons. Protein concentration was determined again by using the BCA assay. The sample was prepared by diluting the metal-bound protein solution with 2% Nitric acid solution for ICP-MS analysis. The metal concentration was determined by using a PE Sciex Elan 9000 ICP-MS instrument and with metal standards from VWR.

2.3.7 Investigating metal Binding Affinity of ZupT by Fluorescence spectroscopy.

Protein samples were prepared in 10mM Bis-Tris buffer, pH7.0, containing 2mM DDM. All buffers were made with metal-free water by passing the water through a Chelex 100 column to remove free metal ions. The sample was excited at 290nm, and the emission scans were taken from 295nm to 500nm. After each addition of metal solution, the sample was mixed and a scan of the sample was recorded. The results were analyzed using KaleidaGraph software to get the fit and determine the metal binding affinity.

2.3.8 Determination of Metal binding affinity of ZupT by Mag-fura-2

The samples were prepared as above. The protein concentration in these experiments was 20uM. First, spectra were recorded from 300nm to 500nm with ~20uM mag-fura2 in 10mM Bis-Tris buffer, pH7.0. Then the protein was added to the sample to make the final concentration ~20uM, and the spectrum recorded again. Then aliquots of metal solution were added, and the spectra recorded after each addition. The absorbance change at 366nm was plotted vs. metal added, and the results analyzed using Dynafit to determine the metal binding affinity.

2.4 Results

2.4.1 ZupT Homology Alignment

The result of a homology alignment using CLUSTALW2 Multiple Sequence Alignment (European Bioinformatics Institute) is shown in Figure 2.3. There are two conserved regions found within the ZupT sequence from different species. These two conserved regions are located in the fourth and fifth transmembrane helices.

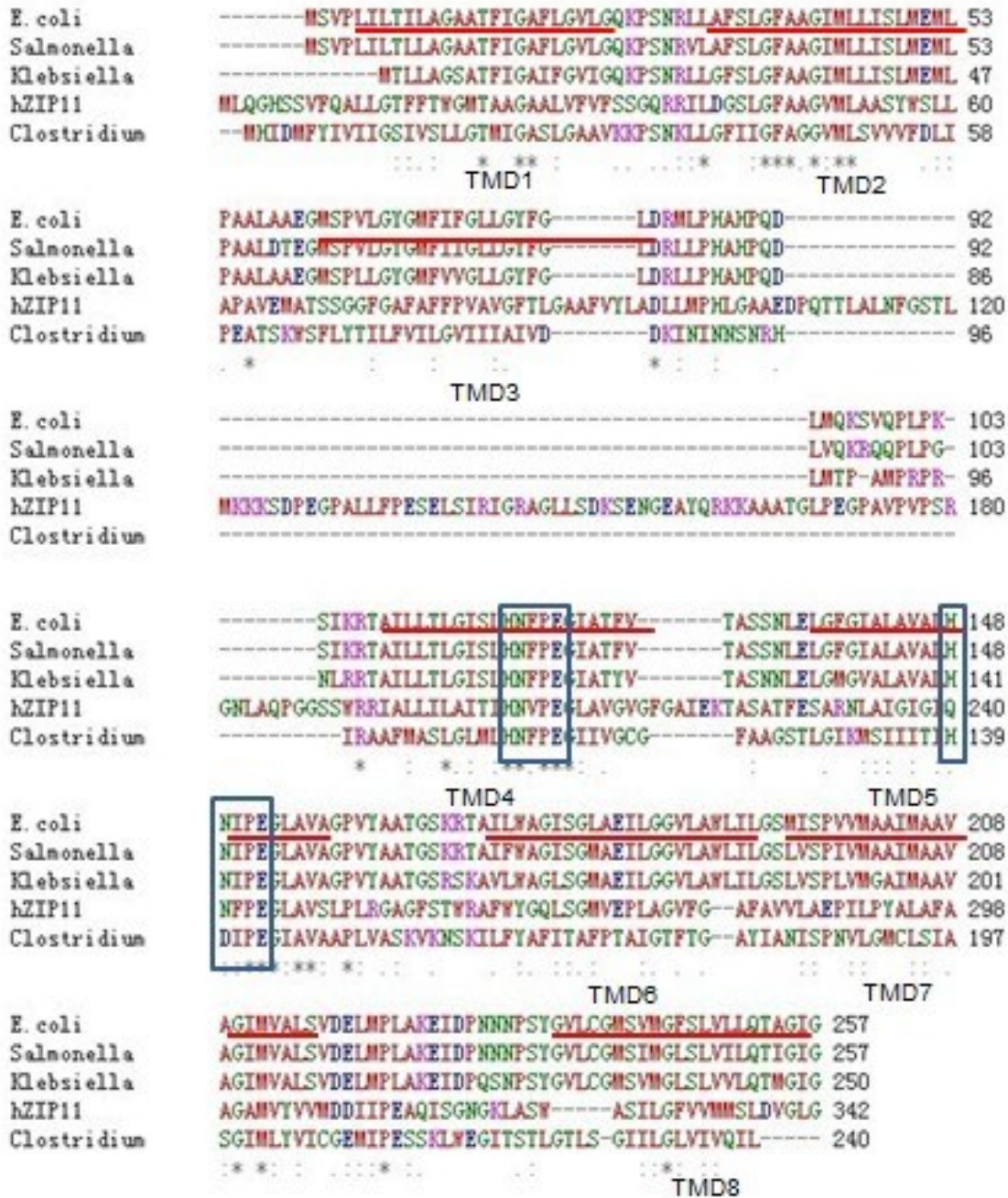


Figure 2.3 Result of a ZupT family sequence alignment, and the conserved regions are framed in boxes.

2.4.2 Optimization of ZupT expression

In our lab, we have several expression systems for ZupT without any affinity tag or with a strep-tag. Table 2.1 lists all the constructs we have for ZupT. I decided to investigate the best expression system for ZupT. As the Western blot results in Figure 2.4 indicate, the best protein expression was from the ZupT pASK IBA3/JM83 in LB medium.

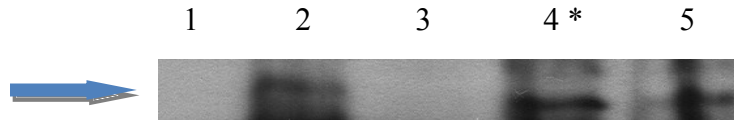


Figure 2.4 Western blot comparing ZupT expression from different systems.

Legend:

Line1: ZupT pASK IBA3/BL21 non-induced in LB medium

Line2: ZupT pASK IBA3/BL21 induced in LB medium

Line3: ZupT pASK IBA3/JM83 non-induced in LB medium

Line4*: ZupT pASK IBA3/JM83 induced in LB medium

Line5: ZupT pASK IBA3/JM83 induced in minimum medium

However, even with this optimized expression system, a clear target band on an SDS-PAGE gel is still not visible (Figure 2.5).

Therefore, further optimization was attempted with different OD_{600} at induction, different concentrations of inducer, different induction temperatures, and different induction times, according to the scheme presented in Table 2.2.

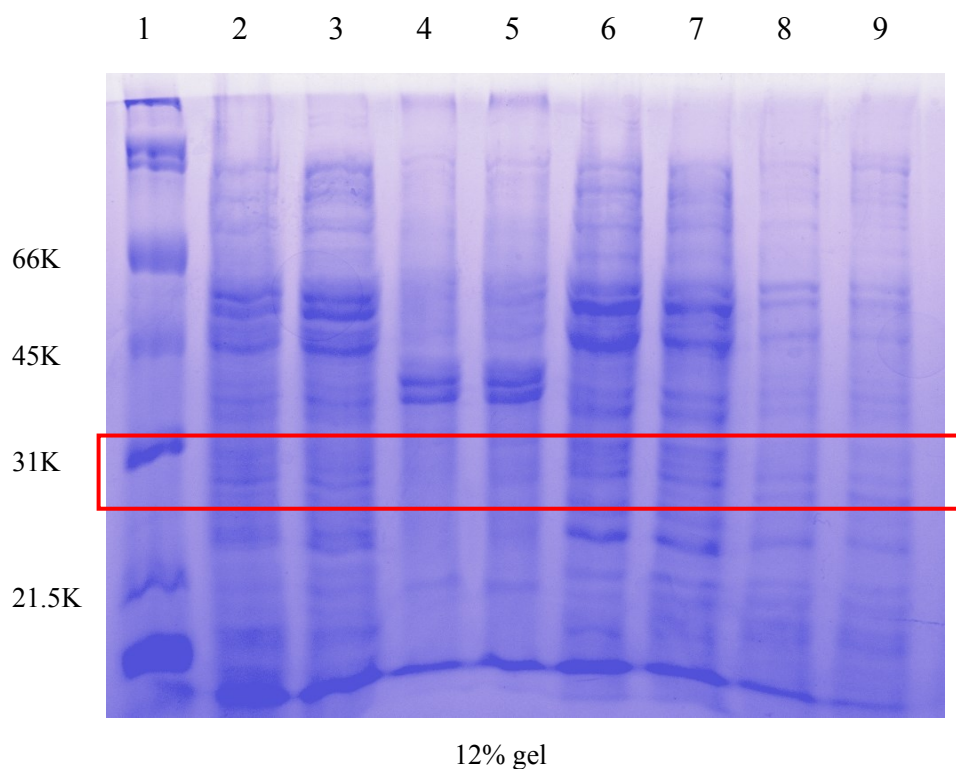


Figure 2.5 Different fractions of noninduced and induced ZupT pASK IBA3/JM83.

Legend:

- Line1: Protein standard
- Line2: Non-induced JM83 low speed supernatant
- Line3: Induced JM83 low speed supernatant
- Line4: Non-induced JM83 low speed pellet
- Line5: Induced JM83 low speed pellet
- Line6: Non-induced JM83 high speed supernatant
- Line7: Induced JM83 high speed supernatant
- Line8: Non-induced JM83 high speed pellet
- Line9: Induced JM83 high speed pellet

Table 2.2 ZupT expression optimization gradient

Strain	Induction OD ₆₀₀	Inducer (anhydrotetracycline (AHT))concentration (ug/L)	Induction temperature(°C)	Induction time (hours)
WT ZupT pASK	0.4	20	16	3, 4, 5
			21	3, 4, 5

IBA3/JM83			30	3, 4, 5
			37	3, 4, 5
		50	16	3, 4, 5
			21	3, 4, 5
			30	3, 4, 5
			37	3, 4, 5
		100	16	3, 4, 5
			21	3, 4, 5
			30	3, 4, 5
			37	3, 4, 5
		200	16	3, 4, 5
			21	3, 4, 5
			30	3, 4, 5
			37	3, 4, 5
	0.6	20	16	3, 4, 5
			21	3, 4, 5
			30	3, 4, 5
			37	3, 4, 5
		50	16	3, 4, 5
			21	3, 4, 5
			30	3, 4, 5
			37	3, 4, 5
		100	16	3, 4, 5
			21	3, 4, 5
			30	3, 4, 5
			37	3, 4, 5

		200	16	3, 4, 5
			21	3, 4, 5
			30	3, 4, 5
			37	3, 4, 5
	0.8	20	16	3, 4, 5
			21	3, 4, 5
			30	3, 4, 5
			37	3, 4, 5
		50	16	3, 4, 5
			21	3, 4, 5
			30	3, 4, 5
			37	3, 4, 5
		100	16	3, 4, 5
			21	3, 4, 5
			30	3, 4, 5
			37	3, 4, 5
		200	16	3, 4, 5
			21	3, 4, 5
			30	3, 4, 5
			37	3, 4, 5
	1.0	20	16	3, 4, 5
			21	3, 4, 5
			30	3, 4, 5
			37	3, 4, 5
		50	16	3, 4, 5
			21	3, 4, 5

			30	3, 4, 5
			37	3, 4, 5
		100	16	3, 4, 5
			21	3, 4, 5
			30	3, 4, 5
			37	3, 4, 5
		200	16	3, 4, 5
			21	3, 4, 5
			30	3, 4, 5
			37	3, 4, 5

The expression level was then checked by western blotting, and part of the results are shown in Figure 2.6. The results suggest that the best condition for this strain is induction at OD₆₀₀ around 0.8, with 200ug/L AHT inducer concentration, and 4 hours of induction at 37 °C. For all subsequent protein expression, these conditions were used.

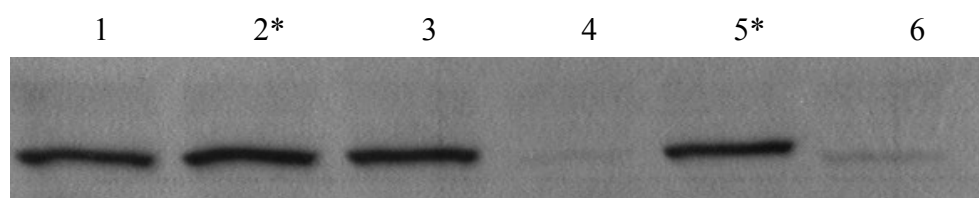


Figure 2.6 Western blotting results for optimization of ZupT expression.

Legend:

Line1: ZupT pASK IBA3/JM83 induced at OD₆₀₀=0.6, induction for 4 hrs at 37°C.

Line2: ZupT pASK IBA3/JM83 induced at OD₆₀₀=0.8, induction for 4 hrs at 37°C.

Line3: ZupT pASK IBA3/JM83 induced at OD₆₀₀=1.0, induction for 4 hrs at 37°C.

Line4: ZupT pASK IBA3/JM83 induced at OD₆₀₀=0.8, induction for 3 hrs at 37°C.

Line5: ZupT pASK IBA3/JM83 induced at OD₆₀₀=0.8, induction for 4 hrs at 37°C.

Line6: ZupT pASK IBA3/JM83 induce at OD₆₀₀=0.8, induction for 5 hrs at 37°C.

2.4.3 ZupT purification

Purification of ZupT proved to be the most difficult part of my project because of the low expression levels. Using a single strep-tactin column, which is specific for any strep-tagged protein, ZupT could not be purified to a high level. Figure 2.7 shows all the fractions during the purification using a single step using a strep-tactin column.

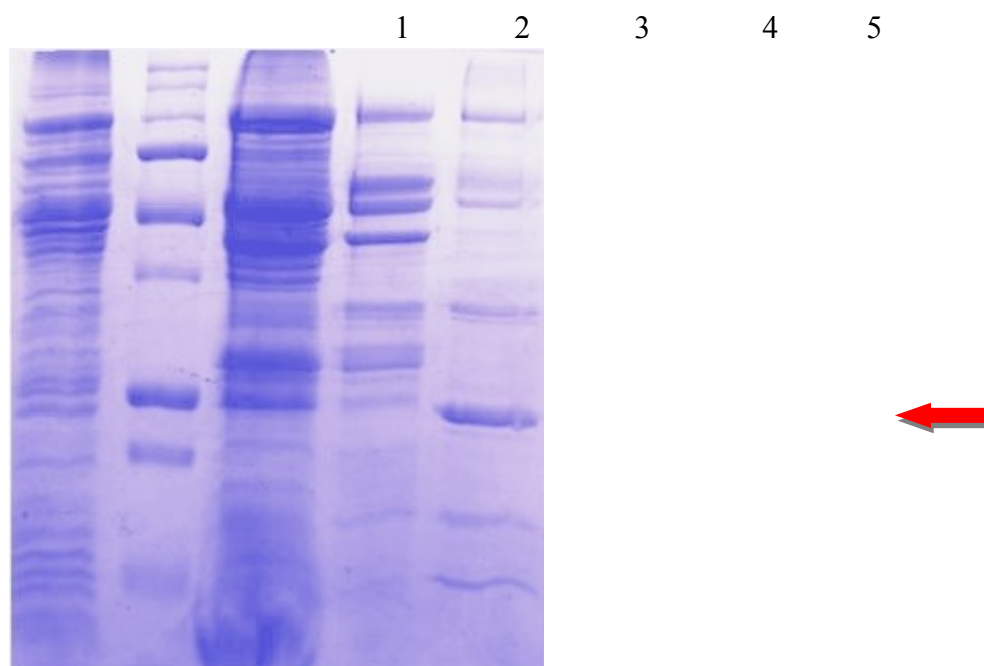


Figure 2.7 SDS gel with the fractions from a ZupT purification using a single strep-tactin column.

Legend:

Line1: High speed Supernatant after detergent solubilization
 Line2: Protein standard
 Line3: Strep-tactin flow-through
 Line4: Strep-tactin wash
 Line5: Final protein eluant

Next, I tried to add additional steps to the purification process: using a combination of a DEAE-Sepharose anion exchange column and strep-tactin column (Figure 2.8), a combination of a Co^{2+} affinity (Talon) column and strep-tactin column (Figure 2.9), and a combination of a Ni^{2+} affinity column and strep-tactin column (Figure 2.10). The combination of the DEAE column and strep-tactin column (Figure 2.8), and the combination of Talon column and strep-tactin column (Figure 2.9) did not give me good quality purified ZupT. However, the combination of a Ni^{2+} column and strep-tactin column gave the best quality purification (Figure 2.10).

When I was developing the purification method, I tried a combination of Co^{2+} -binding Talon column and a strep-tactin column. Surprisingly, I observed that ZupT did not bind to both columns, but it could bind to either of them. The western blotting result (Figure 2.9B) showed that ZupT can bind to the Co^{2+} Talon column. However, after elution it did not bind to the strep-tactin column. When I tried to reverse the order of the columns, strep-tactin first, followed by Talon (Figure 2.9A), the protein could not bind to the Talon column. Perhaps the former result is due a conformation change. When ZupT binds to Co^{2+} , the conformation of ZupT may be changed, and the strep-tag, which is located on the C-terminal end of ZupT, is trapped inside the folded protein. Therefore, it is unable to bind to the strep-tactin column. Alternatively, and more likely, the strep-tag may be cleaved off during binding and elution from a Co^{2+} column. It is unclear in the reverse case, why the partially purified strep-tagged column does not have any binding affinity to Co^{2+} resin. The affinity of ZupT for Co^{2+} should be investigated in the future.

2.4.4 Fluorescence methods to determine the metal-affinity of ZupT

In order to determine the metal-binding affinity of ZupT, the intrinsic tryptophan fluorescence quenching of ZupT when metal solution is added, was utilized. When the environment around a tryptophan residue is changed due to metal binding at a nearby site, its

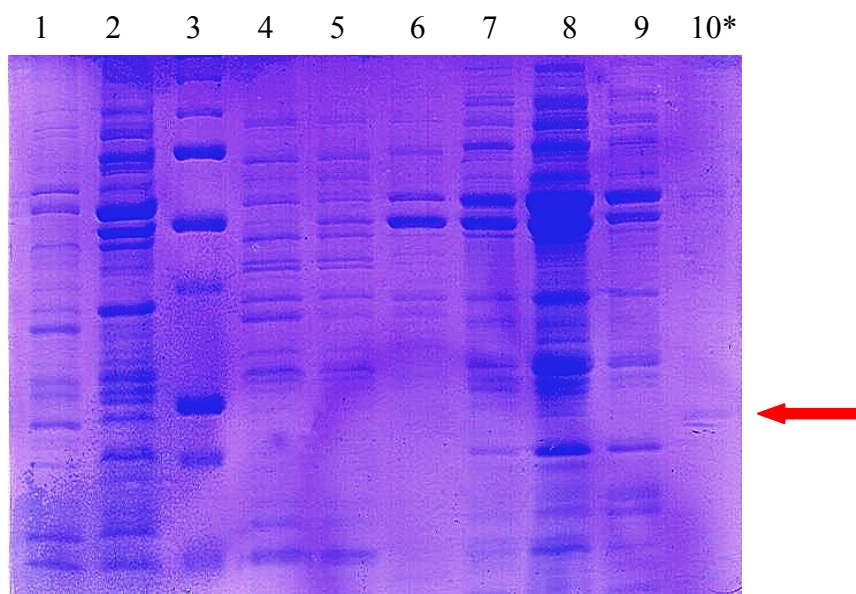


Figure 2.8 SDS gel with the fractions from the ZupT purification for the combination of DEAE ion exchange column and strep-tactin column.

Legend:

- Line1: Low speed supernatant
- Line2: High speed supernatant after detergent solubilization
- Line3: Protein standard
- Line4: DEAE flow-through
- Line5: DEAE wash
- Line6: DEAE 50mM NaCl wash
- Line7: DEAE 200mM NaCl elution
- Line8: Strep-tactin flow-through
- Line9: Strep-tactin wash
- Line10*: Purified ZupT

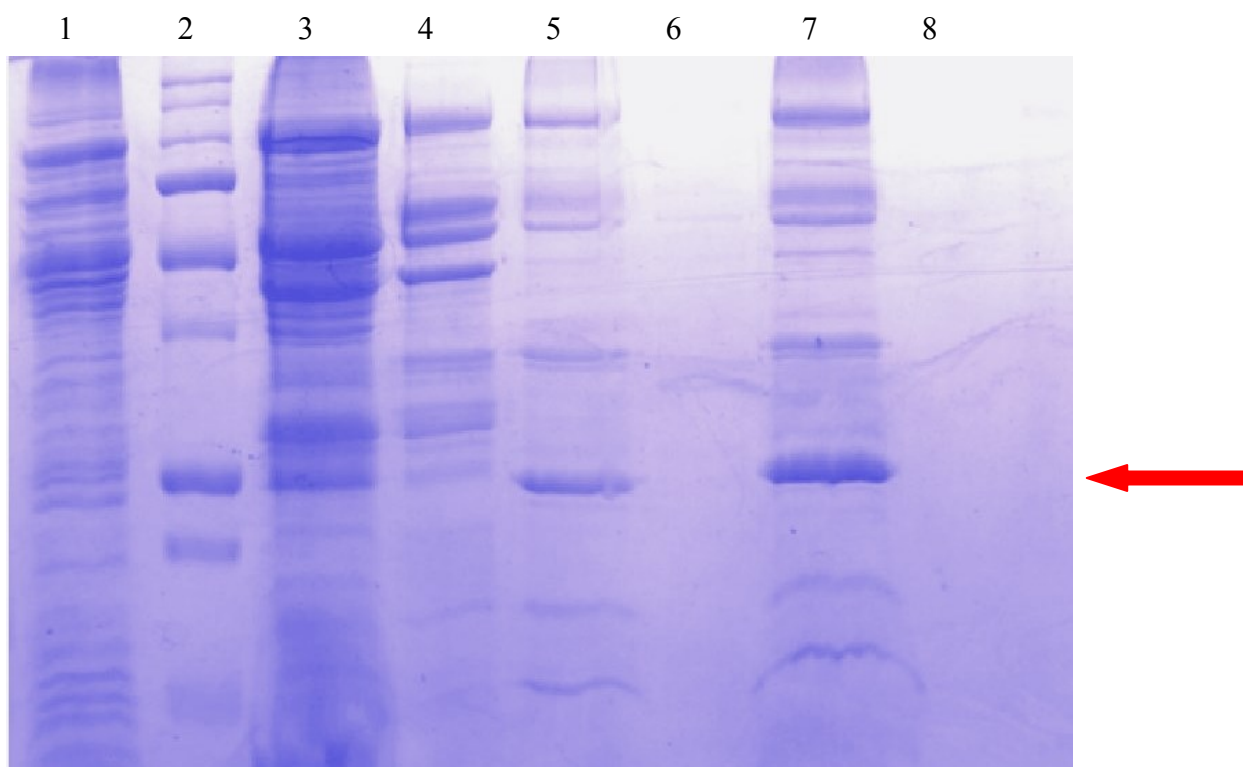


Figure 2.9A. SDS gel with fractions of ZupT purification of combination of Talon column and strep-tactin column. Figure is the result for purification of Strep-tactin followed by Talon column.

Legend:

- Line1: High speed Supernatant
- Line2: Protein standard
- Line3: Strep-tactin flow-through
- Line4: Strep-tactin wash
- Line5: Strep-tactin eluant
- Line6: Talon column flow through
- Line7: Talon column wash
- Line8: 20mM imidazole wash of the Talon column

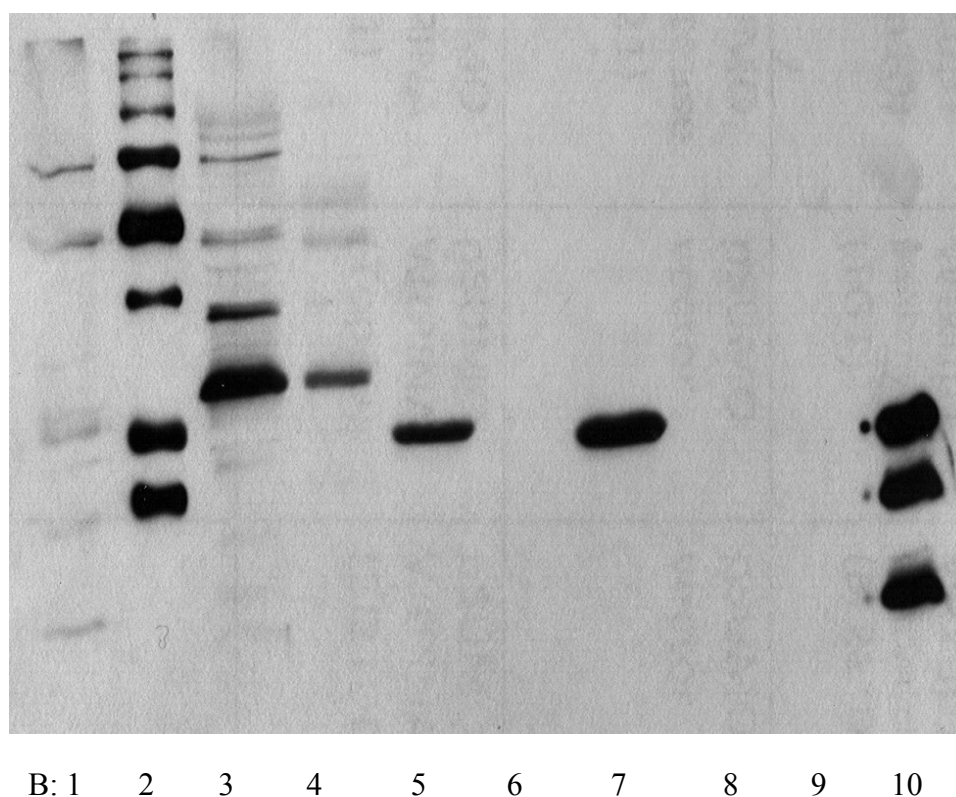


Figure 2.9 B Western blotting results of fractions of ZupT purification of combination of Talon column and strep-tactin column. Figure B is the result for purification of Talon column followed by strep-tactin column.

Legend:

Line1: High speed supernatant
 Line3: Talon column flow through
 Line5: 20mM imidazole wash
 Line7: Strep-tactin flow through
 Line9: Strep-tactin elute

Line2: Protein standards
 Line4: 5mM imidazole wash
 Line6: 75mM imidazole wash
 Line8: Strep-tactin wash
 Line10: Old ZupT -strep tagged protein.

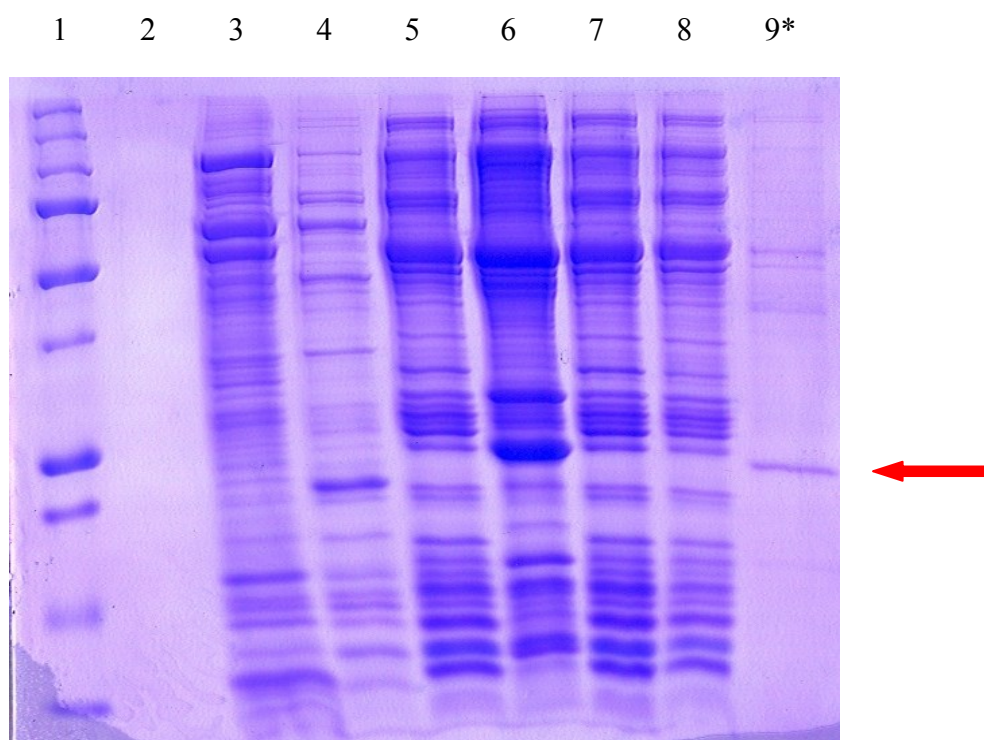


Figure 2.10 SDS gel with the fractions from the ZupT purification of the combination of Ni^{2+} column and strep-tactin column.

Legend:

Line1: protein standard

Line2: Ni^{2+} column flow-through

Line3: Ni^{2+} column wash

Line4: Ni^{2+} column 10mM imidazole wash

Line5: Ni^{2+} column 50mM imidazole wash

Line6: Ni^{2+} column 300mM imidazole wash

Line7: Strep-tactin flow-through

Line8: Strep-tactin wash

Line9*: Purified ZupT

fluorescence signal may change. ZupT has two naturally occurring Trp residues, Trp¹⁷³ and Trp¹⁸⁹. Additionally, the strep tag introduces a third Trp residue at the C-terminus. In this experiment 4uM ZupT in 10uM Bis-tris buffer pH7.0 was used and titrated with increasing concentrations of Zn²⁺. The sample was excited at 290nm.

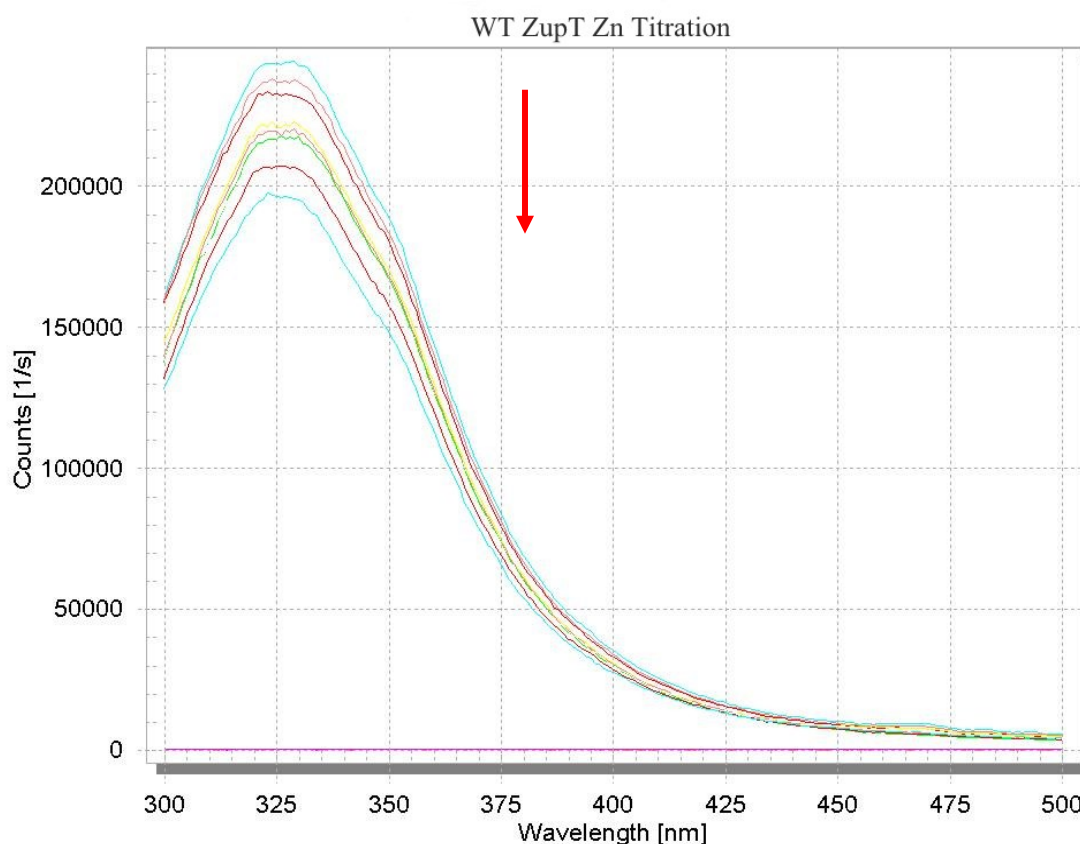


Figure 2.11 Emission spectrum of ZupT in the 300-500nm range with increasing amounts of added Zn²⁺; the arrow shows the direction of fluorescence change.

The relative change in fluorescence emission at 330nm from Figure 2.11 was plotted vs. Zn²⁺ concentration, and the data was fitted using Kaleidagraph software (Figure 2.12). The results suggest that ZupT has only one binding site for zinc since the fluorescence quenching was

essentially complete at one equivalent of added Zn^{2+} , and the K_d of this site is in the low μM range, $1.02 \pm 0.14 \mu\text{M}$.

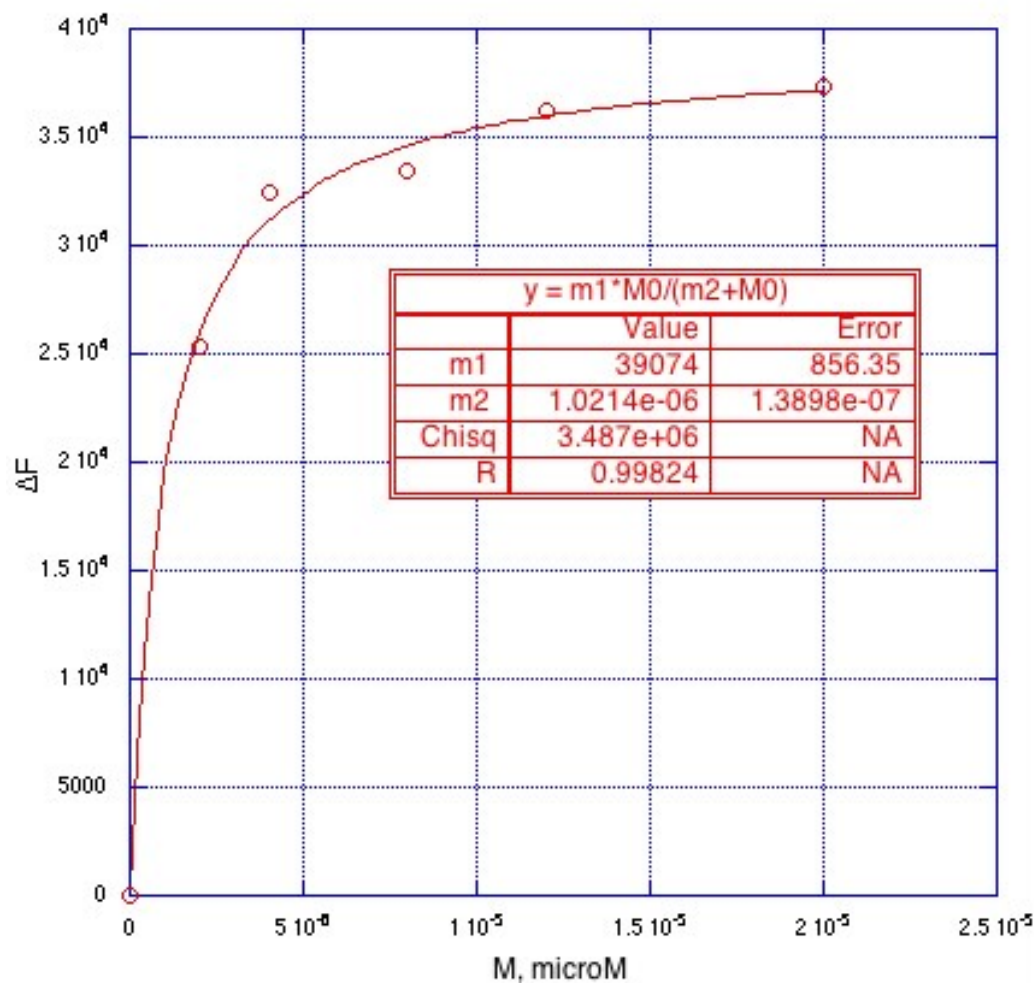


Figure 2.12 Plot of relative change in fluorescence emission at 330nm from Figure 2.11 above as a function of the added zinc salt concentration.

2.4.5 Competition experiments using Mag-fura 2 as a metal-binding competitor of ZupT

Mag-fura2 is a metal indicator, and it has a peak around 366nm without metal ion bound. This peak shifts from 366nm to 325nm when mag-fura2 is bound to divalent metal ions. This indicator was chosen since the affinity results using fluorescence titrations above suggested that

Mag-fura 2 appears to have comparable affinity for metals to ZupT^{73, 74, 75}. In the presence of Mag-fura2, Zn^{2+} and ZupT, Mag-fura2 and ZupT will both compete to bind the metal ion. In order to determine the affinity of ZupT for zinc, the absorbance change at 366nm of mag-fura 2 was monitored in the presence of ZupT and increasing concentration of metal ions, and the data was fitted for a one metal-binding site model to ZupT using DynaFit software (Figure 2.13)^{77, 78}. The K_d from this fit was $0.35 \pm 0.09 \text{ uM}$. The K_d for the indicator, mag-fura 2 used in this fit was 20uM .

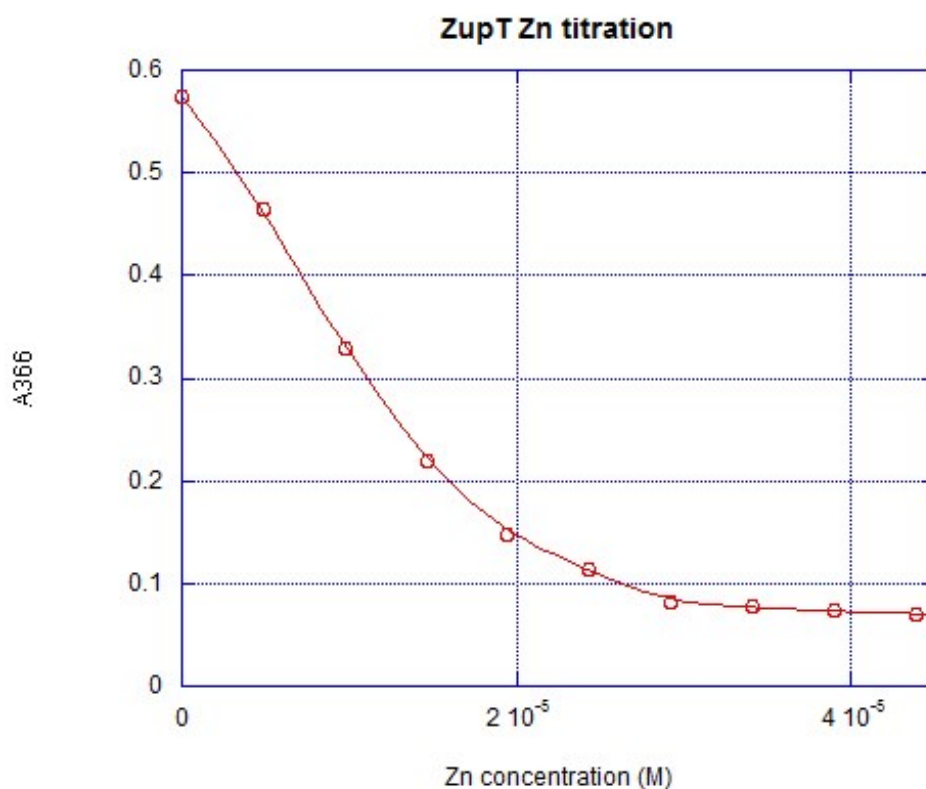


Figure 2.13 Plot the absorbance change at 366 nm of mag-fura-2, and the data was fitted using Dynafit software^{77, 78}.

2.4.6 Stoichiometry of ZupT using ICP-MS

The stoichiometry of ZupT with Zn was determined to be 0.63 ± 0.0 , using a PE Sciex Elan 9000 ICP-MS instrument and with metal standards from VWR.

2.5 Discussion

As a result of this study, a successful purification method has been developed for poorly-expressed membrane proteins that have an intrinsic metal-binding affinity. In this method, a strep-tagged protein without any his-tag, but with low divalent metal affinity, can be purified by using a combination of low affinity binding to Ni^{2+} columns first to remove many impurity proteins, and then a strep-tactin column with the enriched target protein. The low affinity for the Ni^{2+} column is either from the metal binding site, or from some his-rich region in the protein.

It was also observed that heating the protein samples to boiling before loading on SDS gels resulted in protein aggregation and degradation. Many membrane proteins are affected in a similar way; the effect for ZupT was particularly pronounced (Figure 2.13). This suggests that it is possible that some of high molecular weight bands in Figure 2.10 for the purified ZupT sample, may not be other impurity proteins, but perhaps oligomers of ZupT. Although I treated the purified ZupT with simple dilution, DTT and even urea, the upper bands cannot be removed (Figure 2.14). Therefore, if they are oligomers, the oligomers cannot be dissociated easily.

Optimization of ZupT expression was successfully achieved by doing a systematic study to optimize four major expression conditions: induction OD_{600} , inducer concentration, induction temperature, and induction time. Figure 2.5 and 2.6 shows the optimization protocol and part of the western blotting result for optimization of ZupT expression. The western blotting result is interesting: comparing induction after 3 hours, 4 hours, and 5 hours induction at 37°C , there was a surprising difference in the level of protein expression. A reasonable explanation for this

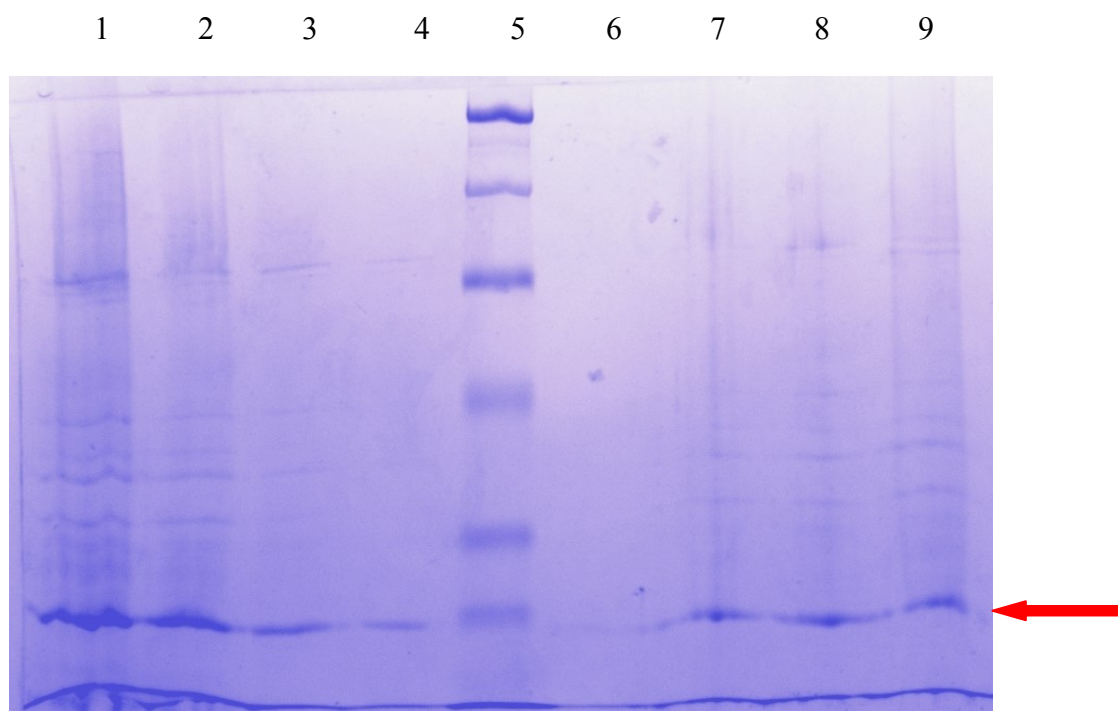


Figure 2.14 10% gel SDS gel result of different treatment of purified ZupT.

Legend:

Line1: 1 time dilution ZupT sample
Line2: 2 time dilution ZupT sample
Line3: 4 time dilution ZupT sample
Line4: 8 time dilution ZupT sample
Line5: Protein standard
Line6: ZupT+1mM DTT
Line7: ZupT+10mM DTT
Line8: ZupT+ 100mM Urea
Line9: ZupT+ 4M Urea

phenomenon is that with 3 hour induction the protein is not expressed very much, 4 hour is the optimum time for induction, after which bacterial proteases degrade most of the overexpressed protein. It is possible that at 5 hours of induction, more ZupT is produced, which results in zinc concentrations in the cytoplasm rising to toxic levels and therefore bacterial proteases degrade the recombinant protein. Also, although colony selection and optimization had been shown to better express His-tagged proteins with different expression systems, it did not work for ZupT pASK IBA3/JM83. Not much difference in expression levels was observed between different colonies in two completely separate experiments. It is likely that overexpression of this transporter is not optimal for cell survival.

All the metal-binding experiments of ZupT were performed at neutral pH, which was reported to be optimum for its binding efficiency⁶⁶. The fluorescence study to measure metal binding of ZupT suggests that ZupT only has one binding site for zinc, and the binding affinity for this site is in the low μM range. The affinity obtained using a direct fluorescence titration, $\sim 1 \mu\text{M}$, and a competition titration experiment using the indicator mag-fura 2, $\sim 0.35 \mu\text{M}$, were in reasonable agreement of each other. Since ZupT is the low-affinity broad spectrum metal transporter that is constitutively expressed in *E. coli*, the binding affinity for zinc looks reasonable. When the environmental zinc concentration is in the low micromolar range or higher, ZupT is adequate for zinc uptake to the cytosol. However, when the environmental zinc concentration is lower than the micromolar range, ZupT may not be able to import zinc, and in this case, the high affinity ZnuABC system is turned on, and used for zinc uptake. The ICP-MS stoichiometry study shows that the stoichiometry of ZupT for Zn is about 0.64, which suggests that there perhaps is one binding site for Zn on ZupT, a result also supported by the binding studies. Usually for one binding site, the stoichiometry should be 1. However, for ZupT the Zn

binding affinity is low, so some Zn may have dissociated during the sample preparation for ICP measurement.

2.7 Further Directions

The importance of the ZIP transporter family is undeniable in all species. Since all the site-specific mutants are ready, these can be now used to map the metal binding site. Also we can determine the metal selectivity of ZupT by using Maga-fura2 indicator competition and fluorescence experiments. The long-term objective of this study is to investigate the human zinc transporters which are homologs of ZupT. If we can understand the basic transport mechanism of ZupT, we can gain fundamental insights into the human zinc transporters.

CHAPTER 3

INVESTIGATING THE METAL BINDING AFFINITY OF PINA-ZNTA

3.1 Purpose

As mentioned in chapter 1, Pineal night-specific ATPase (PINA) is a novel splice variant of the ATP7B gene; defects in ATP7B cause Wilsons disease. Compared to ATP7B, PINA lacks the entire N-terminal domain, which contains six CXXC motifs that are important in copper binding, as well as the first four transmembrane helices. The purpose of this study was to test a similar truncated version of ZntA, PINA-ZntA (Figure 3.1), which lacks the N-terminal domain and the first four transmembrane domains, in order to investigate how the loss of the metal-binding N-terminal domain and the first four transmembrane helices affect the rest of the transporter.

A: ZntA

B: ZntA-PINA

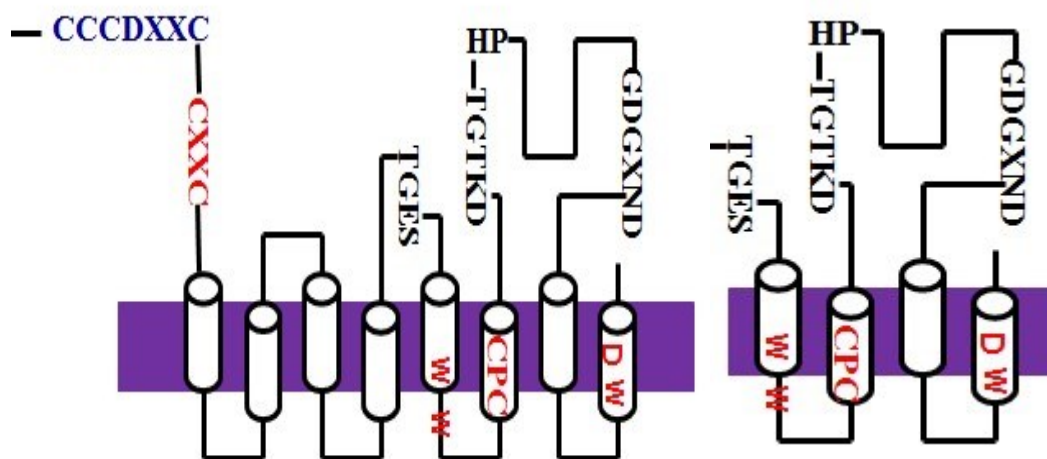


Figure 3.1 Predicted structure of ZntA(A) and PINA-ZntA(B).

3.2 Materials

Plasmid pBAD/myc HisC and E. coli strain LMG194 were purchased from Invitrogen. Strep-tactin resin was purchased from Qiagen.

3.3 Methods

3.3.1 Protein expression and purification of PINA-ZntA

The PINA-ZntA strep/pBAD myc HisC/LMG194 strain was made by a previous lab member. A single colony from LB/Amp plate was used to inoculate 5ml LB culture containing 100ug/ml ampicillin to $OD_{600}=0.10$. 1ml of this culture was used to inoculate 125ml LB culture with 100ug/ml ampicillin and grown overnight at 37°C. 10mL of the overnight LB culture was used to inoculate 1L fresh LB media, and grown at 37°C for about 3.5 hours until the OD_{600} reached 1.0. Then the inducer 0.02% of L-arabinose was added to the culture. After 4 hours induction, the final OD_{600} was still around 1.0. The cells were harvested by centrifugation (8500 rpm, 10 min) and the pellet was stored at -20°C until further use. The pellet was resuspended at 0.2g/mL in buffer A (25mM Tris-Cl pH7.0, 100mM Sucrose, 1mM PMSF, 1mM EDTA and 1mM β -mercaptoethanol (BME)). The cells were lysed by passage through a French press twice at 20,000 p.s.i. Then the cell suspension was incubated with DNaseI (0.02mg/mL) and 2mM $MgCl_2$ at 4°C for 40 minutes to degrade the chromosomal DNA. The debris was removed from the lysed cells by low speed centrifugation (7500rpm, 30 min) at 4°C. The supernatant from the low speed centrifugation was centrifuged again in the ultracentrifuge (45K rpm, 1h) at 4°C to separate the membrane fractions from the soluble part. The pellet from this centrifugation was then resuspended in low ionic strength buffer (1mM Tris-Cl pH7.0, 100mM sucrose, 1mM EDTA, 1mM PMSF, and 1mM β -mercaptoethanol (BME)) to remove the F1-ATPase, and stirred for 1hr at 4°C. The membrane solution was centrifuged again at 45,000 rpm for another 1

hour. Finally, the membrane pellet was stored at 4°C or -20°C till further use. The pellet was resuspended in buffer B (25mM Tris-Cl pH7.0, 100mM Sucrose, 500mM NaCl, 1mM PMSF, 1mM 2-BME) to OD₂₈₀= 100, then Triton X-100 was added to a final concentration 1% and the suspension stirred at 4°C for 1h. After detergent solubilization, the suspension was centrifuged (45Krpm, 40min) to remove the insoluble fractions from soluble proteins. The supernatant from the ultracentrifugation was then loaded on a Ni²⁺ column pre-equilibrated with buffer C (25mM Tris-Cl pH7.0, 100mM Sucrose, 500mM NaCl, 1mM PMSF, 1mM 2-BME, 1mM DDM). The column was then washed with 5 column volumes buffer C, and then the protein containing fractions were eluted with 3 column volumes buffer C with 100mM imidazole. The eluant was concentrated using 30K centricons, and then loaded on a strep-tactin column pre-equilibrated with buffer C. The column was washed with 5 to 10 column volumes buffer C, and then the protein was eluted with 20mL buffer C containing 2.5mM desthiobiotin. 1mL fractions were collected. Protein-containing fractions were combined and concentrated using centricons. In order to remove the desthiobiotin, the protein was passed through a 20ml G-25 column with buffer D (10mM Bis-tris pH7.0, 1mM DDM). The fractions were collected and assayed for protein. All the fractions with protein were pooled and concentrated again using 30K centricons. Finally, the protein solution was aliquoted and stored with 10% glycerol at -80°C till further use.

3.3.2Determination of protein concentration

Protein concentration was determined by using bichinchonic acid assay with bovine serum albumin as standard as discussed in 2.3.5.

3.3.3 Investigating Metal Binding Affinity of PINA-ZntA by Fluorescence spectroscopy.

The protein, in 10mM Bis-Tris buffer pH7.0 containing 1mM DDM, was reduced with 1 mM TCEP for 1 h at 4 °C. The TCEP was removed from the protein solution by passage through a G-25 column. All the buffers and metal solutions were made using metal free water by passing the water through a Chelex 100 column to remove free metal ions. The protein sample was excited at 290nm, and the emission scans were taken from 295nm to 500nm. The results were analyzed using KaleidaGraph software to get the fit and determine the metal binding affinity.

3.3.4 Determination of Metal binding affinity of ZupT by Mag-fura-2

The samples were prepared as above. The protein concentration in these experiments was 10uM. First, spectra were recorded from 300nm to 500nm with ~20uM mag-fura2 in 10mM Bis-Tris buffer, pH7.0. Then the protein was added to the sample to make the final concentration ~10uM, and the spectrum recorded again. Then aliquots of metal solution were added, and the spectra recorded after each addition. The absorbance change at 366nm was plotted vs. metal added, and the results analyzed using Dynafit to determine the metal binding affinity.

3.4 Results

3.4.1 Purification of PINA-ZntA

A previous lab member had trouble purifying PINA-ZntA. Since I was more successful using a metal-affinity column together with the strep-tactin column for ZupT, I applied the same method for PINA-ZntA, which was also a strep-tagged protein. With the combination of Ni²⁺ column and strep-tactin column, good quality purified PINA-ZntA could be obtained (Figure3.2).

3.4.2 Stoichiometry of metal binding to ZntA-PINA by ICP-MS⁷⁶

ICP-MS was used to determine whether ZntA-PINA bound metal ions and the stoichiometry by a previous lab member, Sandhya Muralidharan⁷⁶. It was observed that ZntA-PINA bound all three metal ions, Pb^{2+} , Cd^{2+} , and Zn^{2+} , and the stoichiometry was ~ 0.5 for all three ions.

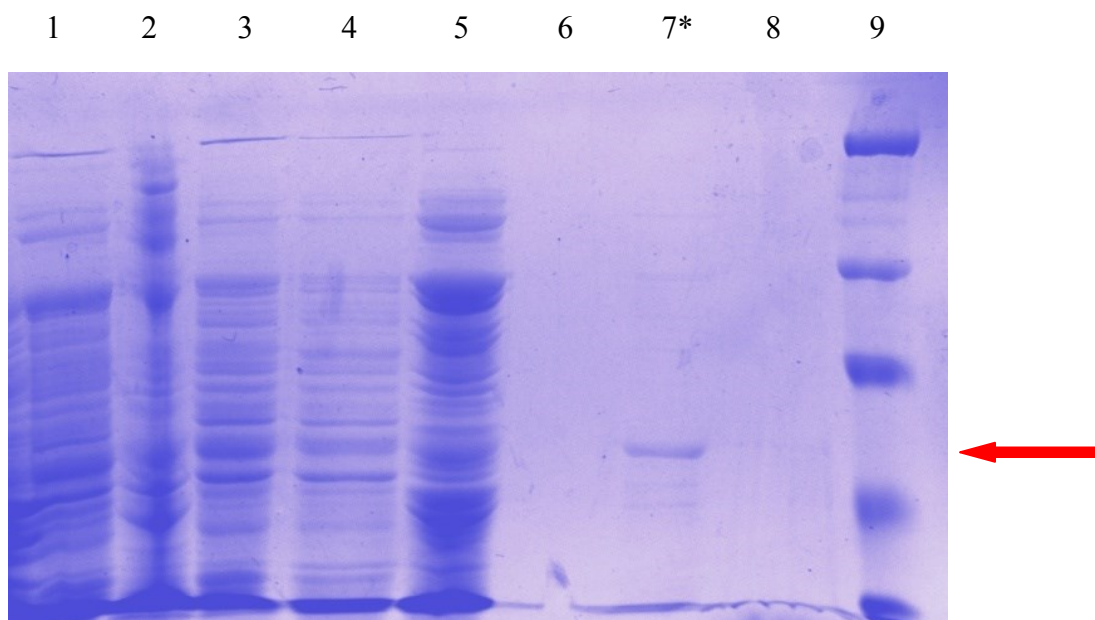


Figure 3.2 SDS gel with the fractions from the PINA-ZntA purification using a combination of Ni^{2+} column and strep-tactin column.

Legend:

Line1: High speed Supernatant

Line2: High speed pellet

Line3: Ni^{2+} flow-through

Line4: Ni^{2+} wash

Line5: Strep flow-through

Line6: Strep wash

Line7: Purified Del231ZntA Strep

Line9: Protein standard

3.4.3 Investigating Metal Binding Affinity of PINA-ZntA by Fluorescence spectroscopy

In order to determine the metal-binding affinity of PINA-ZntA, the intrinsic tryptophan fluorescence quenching of PINA-ZntA was utilized. 4uM PINA-ZntA in 10uM Bis-tris buffer pH7.0, 5 uM TCEP and 1 mM DDM was used in this experiment. The sample was excited at

290nm and the emission scans were taken from 295nm to 500nm. The following figure show the result of fluorescence titration studies of ZntA-PINA with Pb^{2+} (Figure 3.3), Cd^{2+} (Figure 3.4), and Zn^{2+} (Figure 3.5)

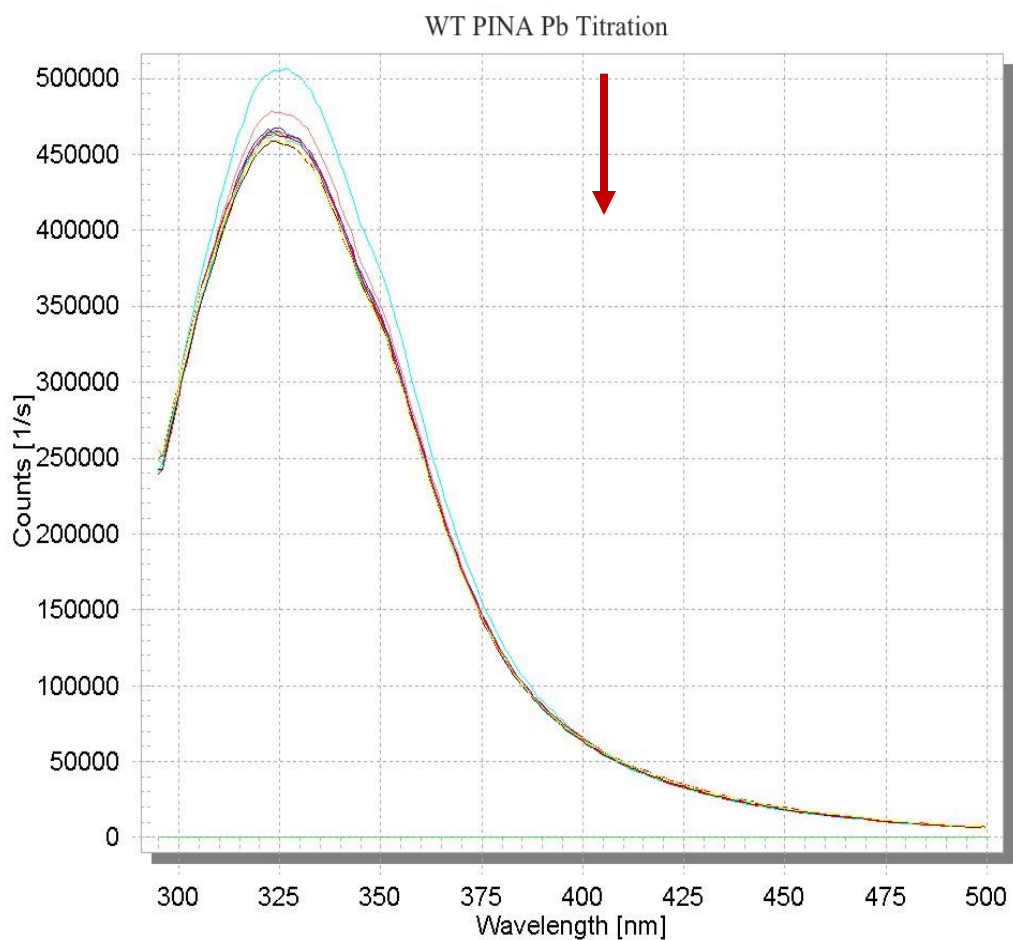


Figure 3.3 Emission spectrum of ZntA- PINA in the 295-500nm range with increasing amounts of added Pb^{2+} ; the arrow indicates the direction of fluorescence change.

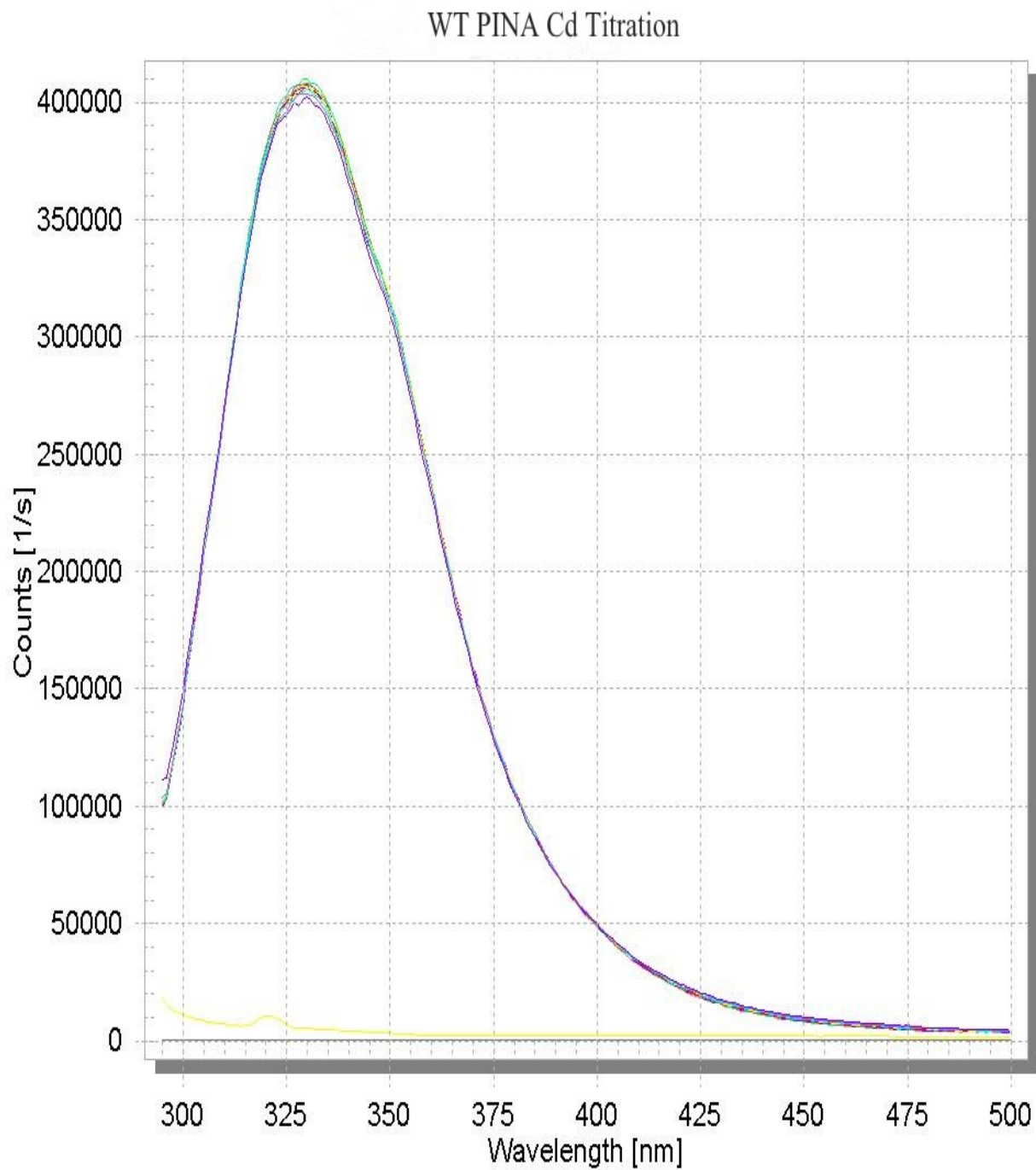


Figure 3.4 Emission spectrum of ZntA- PINA in the 295-500nm range with increasing amounts of added Cd²⁺; there is no observation fluorescence change during the titration.

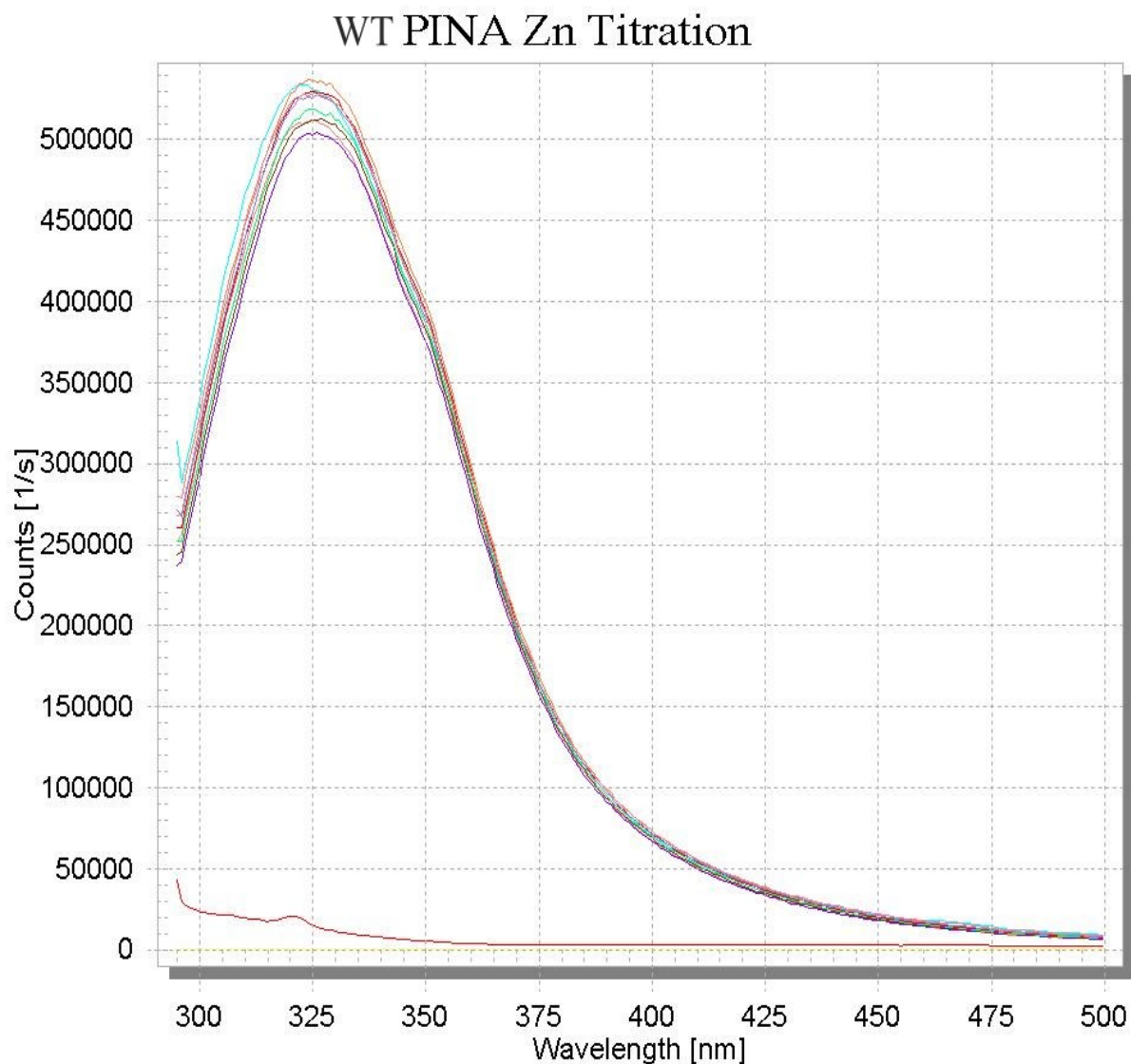


Figure 3.5 Emission spectrum of ZntA- PINA in the 295-500nm range with increasing amounts of added Zn^{2+} , the fluorescence change during the zinc titration was not unidirectional.

Since a fluorescence change was observed for the Pb^{2+} titration, the fluorescence change from Figure 3.3 was plotted vs. added metal concentration in Figure 3.6, and the result suggest that ther stoichiometry of ZntAPINA for Pb^{2+} is ~ 0.5 .

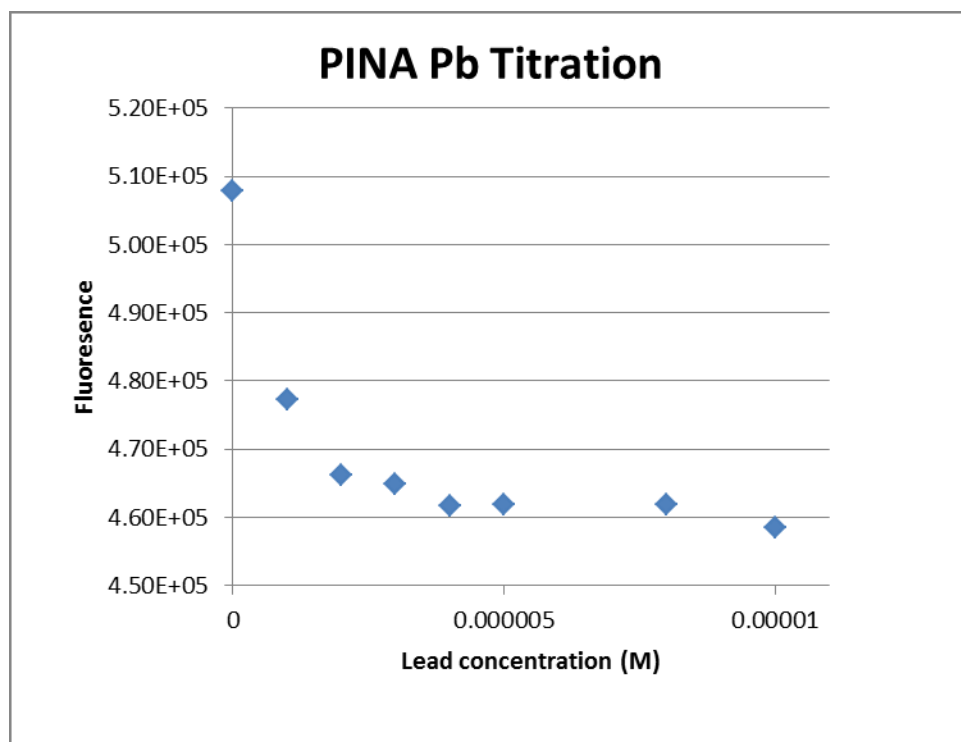
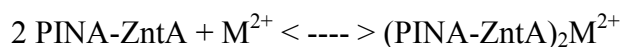


Figure 3.6 Plot of fluorescence change in fluorescence emission at 325nm from Figure 3.3 above as a function of the added lead salt concentration.

3.4.4 Determination of Metal binding affinity of PINA-ZntA by Mag-fura-2

In order to determine the whether PINA-ZntA can bind to zinc and cadmium, mag-fura-2, metal indicator, was used, and the absorbance change at 366nm of mag-fura 2 was monitored in the presence of PINA-ZntA and increasing concentration of Zn^{2+} (Figure 3.6) and Cd^{2+} (Figure 3.7). The data for PINA-ZntA with Zn^{2+} in Figure 3.6 was fitted using DynaFit software^{77, 78}. The data was fitted for a half metal-binding site model to PINA-ZntA:



The K_d obtained from this fit was $(1.5 \pm 0.3) \times 10^{-13} \text{ M}$.

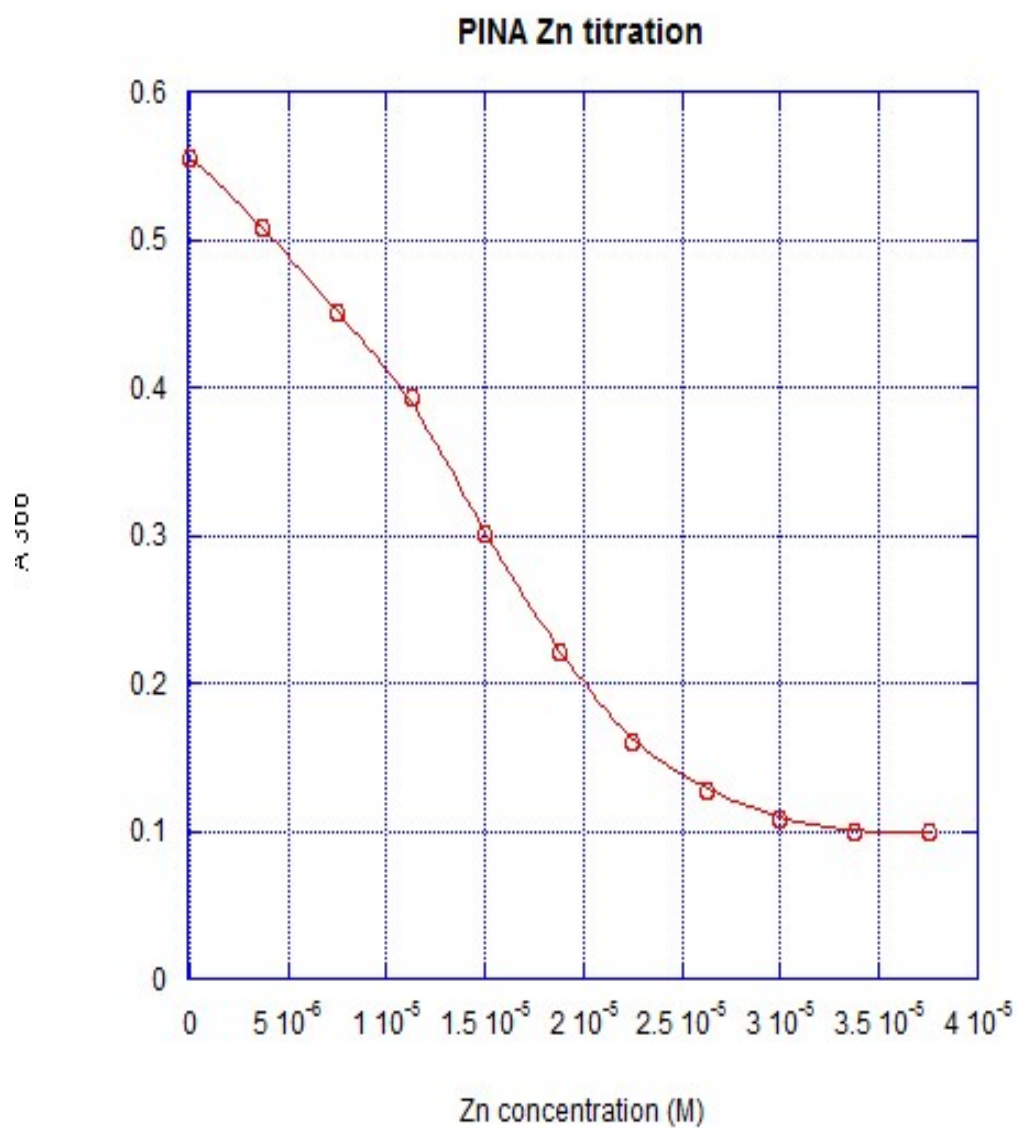


Figure 3.7: Determination of Zn binding affinity of PINA-ZntA using competition titration with mag-fura-2. The absorbance change at 366 nm was plotted, and the data was fitted using Dynafit software^{77, 78}.

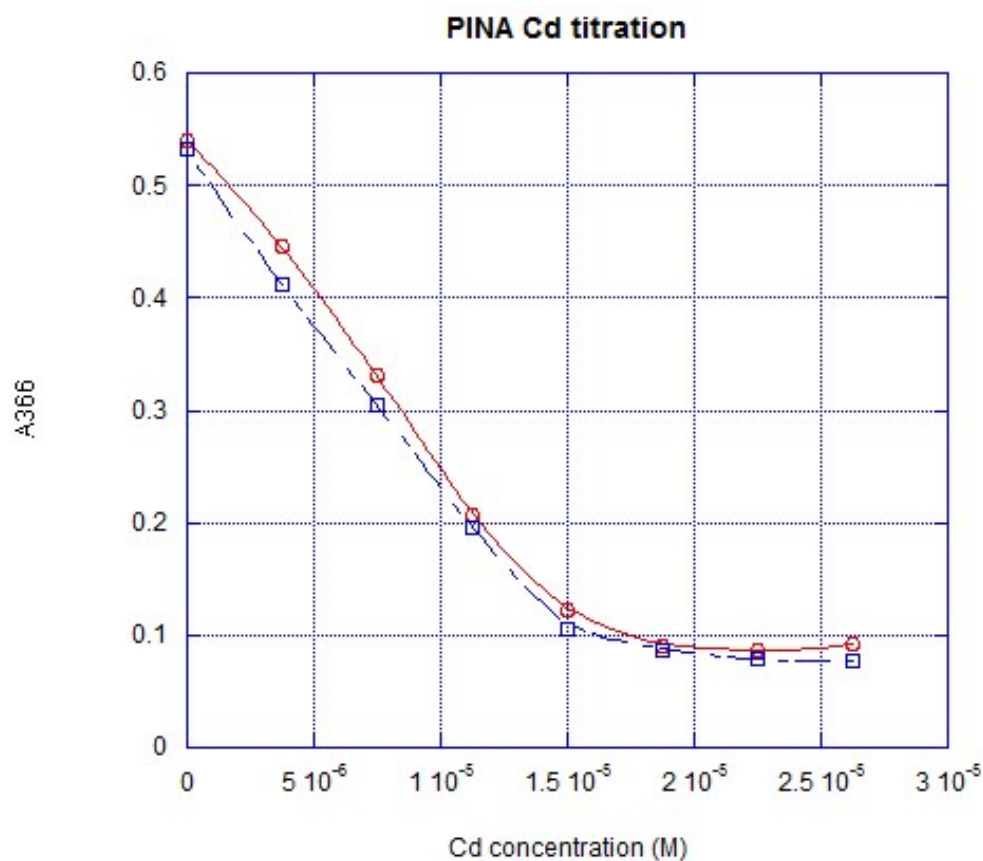


Figure 3.8: Cadmium titration with mag-fura-2 with (red) or without PINA-ZntA present (blue).

As evident from Figure 3.7, there did not appear to be any binding of Cd^{2+} to PINA-ZntA, contrary to our expectations. This was probably due to the protein having been oxidized, resulting in loss of the binding site, during the experiment.

3.5 Discussion

WT ZntA-PINA-strep, a highly truncated protein, was expressed even more poorly than ZupT. Also, with the single strep-tactin column it was hard to get good quality purified protein. I

applied the purification method I developed for ZupT, to purify this protein and got really high quality purified protein as shown in Figure 3.2.

Interestingly, though PINA-ZntA was expressed more poorly than ZupT, with the double column purification method, I was able to obtain better purification than ZupT, though in very low yield. One explanation for this difference is that PINA-ZntA is able to bind to the initial Ni^{2+} column with higher affinity compared to ZupT, and can be washed with higher concentrations of imidazole, and therefore more impurity proteins can be removed at this step.

ZntA-PINA as a truncated transporter shows fluorescence change during fluorescence studies with increasing amount of lead and zinc, but not cadmium. Zinc binding triggered a non-uniform fluorescence change, and cadmium titration did not trigger any change at all. However earlier stoichiometry results indicated that ZntA-PINA can bind to both Zn^{2+} and Cd^{2+} as well as Pb^{2+} . This indicates that binding of Pb^{2+} , Zn^{2+} and Cd^{2+} in PINA-ZntA lead to different changes in the environment around the Trp residues, in contrast to ZntA itself⁷⁶. The ZntA-PINA fluorescence study with Pb^{2+} also shows the half stoichiometry, which supports the previous stoichiometry study results for ZntA-PINA with Pb^{2+} .

The mag-fura-2 results (Figure 3.6 and Figure 3.7) showed that PINA-ZntA can bind to Zn^{2+} , but not Cd^{2+} . However, in previous studies using ICP-MS⁷³, PINA-ZntA does bind Cd^{2+} . It is possible that after removal of the excess TECP, the protein was oxidized during the titration experiments for Cd^{2+} .

The affinity of ZntA-PINA for metal ions was many orders of magnitude greater than that of ZntA itself, with K_d obtained for ZntA-PINA in the range of 10^{-13} M as opposed to 10^{-8} – 10^{-9} M for the metal-binding site in the membrane in wild-type ZntA⁷⁵. Also, the metal-binding site in ZntA-PINA could only bind one metal ion per dimer, in contrast to ZntA with all eight

transmembrane helices intact⁷⁵. This indicates that the first four transmembrane helices, together with the cytosolic portions that were removed in ZntA-PINA either contributes to a full metal-binding site, or helps to organize the structure of the transmembrane helices such that each monomer can bind one metal ion. It is possible that in the PINA variant in humans, Cu⁺ ions are bound much more tightly than in the full-length ATP7B protein. The physiological reason for this is yet to be understood.

3.6 Further Direction

The fluorescence study shows that ZntA-PINA is able to bind metals but suggests that in contrast to ZntA, the different metals may have different ligands in this truncated mutant, which result in different changes in the environment around the Trp residues. Future studies will be aimed at identifying the metal-binding residues for each metal ion, using site-specific mutagenesis.

Studies for PINA-ZntA are also important in showing that PINA has metal-binding capability. This indicates that the PINA splice variant of ATP7B in humans may also be able to bind copper ions but with a much higher affinity.

REFERENCES

1. Roat-Malone, R. M. (2008) Bioinorganic Chemistry: a short course, 2nd ed., John Wiley and sons, USA.
2. Bruce A. Averill (2007), general chemistry principles patterns and applications, v.1.0, Flat world knowledge.
3. M. Indriati Hood, (2012), Nutritional immunity: transition metals at the pathogen–host interface, Nature Reviews, Microbiology.
4. E.G., and Raymond, K.N. (1994), Transition-metal storage, transport, and biomineralization.
5. Christos T. Chasapis (2012), Zinc and human health: an update, Arch Toxicol
6. Sergi Puig, Placing metal micronutrients in context: transport and distribution in plants; 2009, Current Opinion in Plant Biology.
7. Muysen, Brita, T. A.; De Schamphelaere, Karel A. C.; Janssen, Colin R. (2006). "Mechanisms of chronic waterborne Zn toxicity in *Daphnia magna*". Aquatic Toxicology
8. Varsha Mudgal, Effect of Toxic Metals on Human Health, The Open Nutraceuticals Journal, 2010
9. Shankar, A.H. & Prasad A.S. 1998. Zinc and immune function: the biological basis of altered resistance to infection. *Am. J. Clin. Nutr.*, 68(suppl.): 447S-463S
10. Hambidge, K.M. 1987. Zinc. In: *Trace elements in human and animal nutrition*. Mertz, W., ed. 5th, Vol. 1., p.1-137. Orlando, Florida, Academic Press, Inc.
11. Rink, L.; Gabriel P. (2000). "Zinc and the immune system". *Proceedings of the Nutrition Society (2000)*
12. Laura M. Plum (2010), The Essential Toxin: Impact of Zinc on Human Health, *International Journal of Environmental Research and Public Health*.

13. Ho, E (2001), Dietary zinc supplementation inhibits NFkappaB activation and protects against chemically induced diabetes in CD1 mice. *Exp Biol Med (Maywood)*
14. Terres-Martos, C (1998), Serum Zinc and copper concentrations and Cu/Zn ratios in patients with hepatopathies or diabetes. *J trace Elem Med Biol.*
15. Fosmire, G. J. (1990). "Zinc toxicity". *American Journal of Clinical Nutrition*
16. Frederickson, C.J.(2005), The neurobiology of zinc in health and disease. *Nat Rev Neurosci.*
17. Nicold T. Watt (2011), the role of Zinc in Alzheimer's disease, *International Journal of Alzheimer's disease.*
18. Adlard, P.A.(2008), Rapid restoration of cognition in Alzheimer's transgenic mice with 8-hydroxy quinolone analogs is associated with decreased interstitial Abeta. *Neuron.*
19. Grass,G (2002), ZupT is a Zn(II) uptake system in Escherichia coli, *J bacterial.*
20. Mourad Sabri(2008), Roles of the Extraintestinal Pathogenic Escherichia coli ZnuACB and ZupT Zinc Transporters during Urinary Tract Infection.
21. C.E. Outten, T.V. O'Halloran(2001), Femtomolar sensitivity of metalloregulatory proteins controlling zinc homeostasis, *Science* 292 (2001) 2488–2492
22. C.W. MacDiarmid, L.A. Gaither, D. Eide, Zinc transporters that regulate vacuolar zinc storage in *Saccharomyces cerevisiae*, *EMBO J.* 19 (2000) 2845–2855
23. R.D. Palmiter, S.D. Findley, Cloning and functional characterization of a mammalian zinc transporter that confers resistance to zinc, *EMBO J.* 14 (1995) 639–649

24. D.A. Suhy, K.D. Simon, D.I. Linzer, T.V. O'Halloran, Metallothionein is part of a zinc-scavenging mechanism for cell survival under conditions of extreme zinc deprivation, *J. Biol. Chem.* 274 (1999) 9183–9192
25. C.J. Frederickson, S.W. Suh, D. Silva, C.J. Frederickson, R.B. Thompson, Importance of zinc in the central nervous system: the zinc-containing neuron, *J. Nutr.* 130 (2000) 1471S–1483S.
26. L.C. Costello, R.B. Franklin, Novel role of zinc in the regulation of prostate citrate metabolism and its implications in prostate cancer, *Prostate* 35 (1998) 285–296.
27. David J. Eide, Zinc transporters and the cellular trafficking of zinc, *Biochimica et Biophysica Acta* 1763(2006) 711-722.
28. K. Hantke, Bacterial zinc transporters and regulators, *BioMetals* 14 (2001) 239-249.
29. K. Hantke, Bacterial zinc uptake and regulators, *Current Opinion in Microbiology* 8 (2005) 196-202.
30. Juan P. Liuzzi, Mammalian zinc transporters, *Annual Review of Nutrition* 24 (2004) 72-151.
31. L. A. Gaither, Eukaryotic zinc transporters and their regulation. *Biomaterials* 14 (2001) 251-270
32. N. Grotz, Identification of a family of zinc transporter genes from *Arabidopsis* that respond to zinc deficiency. *Proc. Natl. Acad. Sci. USA* 95 (1998) 7220-7224
33. H. Zhao, The ZRT2 gene encodes the low affinity zinc transporter in *Saccharomyces cerevisiae*. *J. Biol. Chem.* 271 (1996) 23203-23210
34. H. Zhao, The yeast ZRT1 gene encodes the zinc transporter protein of a high-affinity uptake system induced by zinc limitation. *Proc. Natl. Acad. Sci. USA* 93 (1996) 2454-2458

35. D. J. Eide, the SLC39 family of metal ion transporters, *Pflugers Arch.* 447 (2004) 796-800
36. M. L. Guerinot, the ZIP family of metal transporters. *Biochim. Biophys. Acta.* 1465 (2000) 190-198
37. B. H. Eng, Sequence analyses and phylogenetic characterization of the ZIP family of metal ion transport proteins, *J. Membr. Biol.* 166 (1998) 1-7
38. E. E. Roger, Altered selectivity in an Arabidopsis metal transporter. *Proc. Natl. Acad. Sci. USA* 97 (2000) 12356-12360
39. K. M. Taylor, The LZT proteins; the new LIV-1 subfamily of zinc transporters. *Biochim. Biophys. Acta Biomembr.* 1611 (2003) 16–30
40. N. A. Begum, Mycobacterium bovis BCG cell wall and lipopolysaccharide induce a novel gene, BIGM103, encoding a 7-TM protein: Identification of a new protein family having Zn-transporter and Zn-metalloprotease signatures. *Genomics* 80 (2002) 630-645
41. J. Lasswell, Cloning and characterization of IAR1, a gene required for auxin conjugate sensitivity in Arabidopsis. *Plant Cell* 12 (2000) 2395-2408
42. I. T. Paulsen, A novel family of ubiquitous heavy metal ion transport proteins. *J. Membr. Biol.* 156 (1997) 99-103
43. M. L. Guerinot, Zeroing in on zinc uptake in yeast and plants. *Curr. Opin. Plant Biol.* 2 (1999) 244-249
44. R. J. McMahon, Mammalian zinc transporters. *J. Nutr.* 128 (1998) 667-670
45. R. J. Cousins, Integrative aspects of zinc transporters. *J. Nutr.* 130 (2000) 1384S0-1387S

46. E. D. Harris, Cellular transporters for zinc. *Nutr. Rev.* 60 (2002) 121-124
47. M. Bramkamp, Common patterns and unique features of P-type ATPases: a comparative view on the KdpFABC complex from *Escherichia coli*. *Mol. Membr. Biol.* 24 (2007) 375-386
48. F. Di Leva, The plasma membrane Ca^{2+} ATPase of animal cells: structure, function, and regulation. *Arch. Biochem. Biophys.* 476 (2008) 65-74
49. G. Duby, The plant plasma membrane proton pump ATPase: a highly regulated P-type ATPase with multiple physiological roles. *Pflügers Arch.* 457 (2009) 645-655
50. C. Toyoshima, Crystal structure of the calcium pump of sarcoplasmic reticulum at 2.6 Å resolution. *Nature* 405 (2000) 647-655
51. W. Kuhlbrandt, Biology, Structure and Mechanism of P-type ATPases, *Nature* 5 (2004) 282-294.
52. T. L. Sorensen, Localization of a K^{+} -binding site involved in dephosphorylation of the sarcoplasmic reticulum Ca^{2+} ATPase. *F. Biol. Chem.* 279 (2004) 46355-46358
53. C. Toyoshima, Structural changes in the calcium pump accompanying the dissociation of calcium. *Nature* 418 (2002) 605-611
54. S. Fahn, Sodium-potassium-activated adenosine triphosphatase of electrophorus electric organ. V. phosphorylation by adenosine triphosphate- ^{32}P . *F. Biol. Chem.* 243 (1968) 1993-2002
55. R. L. Post, A phosphorylated intermediate in adenosine triphosphate dependent sodium and potassium transport across kidney membranes. *F. Biol. Chem.* 240 (1965) 1437-1445
56. R. Whittam, Transport across cell membranes. *Annu. Rev. Physiol.* 32 (1970) 21-60
57. J. E. Hall, Textbook of medical physiology St. Louis, 2006.

58. K. B. Axelsen, Evolution of substrate specificities in the P-type ATPase superfamily, *J. Mol. Evol.* 46 (1998) 84-101
59. A. Anton, CzcD is a heavy metal ion transporter involved in regulation of heavy metal resistance in *Ralstonia* sp. Strain CH34. *J. Bacteriol* 181 (1999) 6876-6881
60. E. H. Kim, Switch or Funnel: How RND-Type Transport Systems Control Periplasmic Metal Homeostasis, *Journal of Bacteriology* 193 (2011) 2381-2387
61. P. M. Jones, ABC transporters: a riddle wrapped in a mystery inside an enigma, *Trends Biochem Sci* 34 (2009) 520-531
62. D. K. Blencowe, Zn (II) metabolism in prokaryotes, *FEMS Microbiol Rev* 27 (2003) 291-311
63. D. K. Blencowe, Zn (II) metabolism in prokaryotes, *FEMS Microbiol Rev* 27 (2003) 291-311
64. C. Rensing, and B. Mitra, Zinc, Cadmium, and Lead resistance and Homeostasis, In *Molecular Microbiology of Heavy Metals* (2007) 321-341
65. G. Grass, The metal permease ZupT from *Escherichia coli* is a transporter with a broad substrate spectrum, *J. Bacteriol* 187 (2005) 1604-1611
66. N. Taudte, Point mutations change specificity and kinetics of metal uptake by ZupT from *Escherichia coli*, *Biometals* 23 (2010) 643-656
67. J. Liu, Metal-binding affinity of the transmembrane site in ZntA: implications for metal selectivity, *Biochemistry* 45 (2006) 763-772.
68. J. Borjigin, A novel pineal night-specific ATPase encoded by the Wilson disease gene, *J Neurosci* 19 (1999) 1018-1026.

69. M. Macchi, Human pineal physiology and functional significance of melatonin. *Front Neuroendocrinol* **25** (2004): 177–95
70. A. Ala, Wilson's disease. *Lancet* **369** (2007): 397–408
71. Rensing C, The zntA gene of Escherichia coli encodes a Zn(II)-translocating P-type ATPase, *Proc Natl Acad Sci U S A*(1997) 94(26):14326-31
72. Z. Hou, The metal specificity and selectivity of ZntA from Escherichia coli using the acylphosphate intermediate, *J Biol Chem* (2003) 278 (31) 28455-61
73. S.J. Dutta, Conservative and nonconservative mutations of the transmembrane CPC motif in ZntA: effect on metal selectivity and activity, *Biochemistry* (2007) 24 (12) 3692-73
74. J. Liu, Metal-binding characteristics of the amino-terminal domain of ZntA: binding of lead is different compared to cadmium and zinc, *Biochemistry* 2005; 44: 5159–5167.
75. J. Liu, Metal-binding affinity of the transmembrane site in ZntA: implications for metal selectivity, *Biochemistry*, 2006;45:763–772
76. S. Muralidharan, Investigating the metal binding sites in ZntA, a zinc transporting ATPase, Wayne State University. Digital Commons, 2010.
77. K.H. Scheller, Metal Ion/Buffer Interactions. *Eur. J. Biochem.* 1980; 107, 455-466
78. T. J. Simons Measurement of free Zn²⁺ ion concentration with the fluorescent probe mag-fura-2 (furaptra), *J. Biochem. Biophys.*(1993) Methods 27, 25-37

ABSTRACT**INVESTIGATING THE METAL BINDING AFFINITY OF BACTERIAL ZINC TRANSPORTERS:
ZUPT AND TRUNCATED ZNTA (ZNTA-PINA)**

by

FEI NIE**August 2013****Advisor:** Dr. Bharati Mitra**Major:** Biochemistry and Molecular Biology**Degree:** Master of Science

Zinc is essential trace elements for all living organisms and serves as cofactor and structural cofactors for more than 300 enzymes. ZupT is one of the members of ZIP super family of transporter proteins, which were identified as iron and zinc transporter in Eukaryotes at first. However, recent evidence showed that some of members can also transport other metal ions, such as manganese or cadmium, and ZIP proteins also exist in bacteria. ZupT is responsible for zinc uptake in *E. coli*; however, its full metal selectivity is not yet characterized. In addition, the mechanism of transport is also unknown. Therefore, my goal is to check the affinity of ZupT with different metal ions, and try to define the metal binding site by testing different mutants.

AUTOBIOGRAPHICAL STATEMENT

08/2005-07/2009: Bachelor of Science (Hons.), Biotechnology, Dalian Medical University

09/2008-05/2011: Study as an exchange student in Laramie County Community College, USA

09/2011-08/2013: Master, Biochemistry and Molecular Biology, School of Medicine, Wayne State University, USA